THE INVESTIGATION OF THE ADDITION OF TiO_2, TiN, TiC OF MICRO ARC OXIDATION COATING ON AZ31 ALLOY

2022
MASTER THESIS
METALLURGICAL AND MATERIALS ENGINEERING

Abubaker Ibrahim ELSADAWI

Thesis Advisor
Assoc. Prof. Dr. Fatih AYDIN

THE INVESTIGATION OF THE ADDITION OF TiO_2, TiN, TiC OF MICRO ARC OXIDATION COATING ON AZ31 ALLOY

Abubaker Ibrahim ELSADAWI

T.C.
Karabuk University
Institute of Graduate Programs
Department of Metallurgical and Materials Engineering
Prepared as
Master Thesis

Thesis Advisor
Assoc.Prof.Dr. Fatih AYDIN

KARABUK

September 2022

I certify that in my opinion the thesis submitted by Abubaker Ibrahim ELSADAWI titled "THE INVESTIGATION OF THE ADDITION OF TiO_2, TiN, TiC OF MICRO ARC OXIDATION COATING ON AZ31 ALLOY" is fully adequate in scope and in quality as a thesis for the degree of Master of Science.

Assoc. Prof. Dr. Fatih AYDIN .....
Thesis Advisor, Department of Metallurgical and Materials Engineering

This thesis is accepted by the examining committee with a unanimous vote in the Department of Metallurgical and Materials Engineering as a Master of Science thesis. September 23, 2022

Examining Committee Members (Institutions)	Signature
Chairman : Assoc. Prof. Dr. Yüksel AKINAY (YYU)	…….
Member : Assoc. Prof. Dr. Fatih AYDIN (KBU)	.....
Member : Assist. Prof. Dr. İsmail Hakkı KARA (KBU)	.....

The degree of Master of Science by the thesis submitted is approved by the Administrative Board of the Institute of Graduate Programs, Karabuk University.

Prof. Dr. Hasan SOLMAZ .....
Director of the Institute of Graduate Programs

"I declare that all the information within this thesis has been gathered and presented in accordance with academic regulations and ethical principles and I have according to the requirements of these regulations and principles cited all those which do not originate in this work as well."

Abubaker Ibrahim ELSADAWI

ABSTRACT

M. Sc. Thesis

THE INVESTIGATION OF THE ADDITION OF TiO_2, TiN, TiC OF MICRO ARC OXIDATION COATING ON AZ31 ALLOY

Abubaker Ibrahim ELSADAWI

Karabük University
Institute of Graduate Programs
The Department of Metallurgical and Materials Engineering

Thesis Advisor:
Assoc. Prof. Dr. Fatih AYDIN
September 2022, 55 pages

Magnesium and its alloys have very important specifications for the manufacture of products that require a decrease in the weight of the product, which leads to a decrease in energy consumption, with high specific strength and high vibration damping properties. However, its poor resistance to corrosion and wear is what most limits the scope of its applications. This made the researchers focus on finding a solution to this problem. One of the solutions adopted by the researchers is the coating, and one of the techniques used in the coating of magnesium alloy is micro-arc oxidation coating, which is what this project will be based on coating AZ31 Mg alloy. This alloy is widely produced and has a wide variety of uses. In this project, the effect of adding TiO_2, TiN, and TiC to the MAO coating of AZ31 alloy will be studied. It is the first study on the effects of adding TiO_2, TiN, and TiC to the MAO coating of AZ31 alloy. So, these compounds will be added to the electrolyte solution and their effects on improving the alloy's resistance to corrosion and wear will be studied through MAO technology.

After coating, SEM, XRD, XPS, FTIR, Raman analyses were utilized to characterize the morphology, phase analysis and chemical composition of the surfaces. Through electrochemical corrosion experiments (electrochemical impedance, potentiodynamic), the corrosion properties of the coating were examined. The project aims to dramatically improve the AZ31 alloy's corrosion and wear resistance by adding TiO_2, TiN, and TiC to MAO technology. In addition to the conclusion of the study and the results that will be achieved, the areas of use of magnesium alloys will also increase. The thesis will contribute to providing a database for researchers and new scientific articles in the same field.

Key Words : Micro arc oxidation, AZ31 alloy, corrosion, wear.
Science Code : 91510

ÖZET

Yüksek Lisans Tezi

AZ31 ALAŞIMININ MİKRO ARK OKSİDASYON KAPLAMASINA TiO_2, TiN, TiC İLAVESİNİN ARAŞTIRILMASI

Abubaker Ibrahim ELSADAWI

Karabük Üniversitesi
Lisansüstü Eğitim Enstitüsü
Metalurji ve Malzeme Mühendisliği Anabilim Dalı

Tez Danışmanı:
Doç. Dr. Fatih AYDIN
Eylül 2022, 55 sayfa

Magnezyum ve alaşımları, yüksek özgül mukavemet ve yüksek titreşim sönümleme özelliklerine sahip, ürün ağırlığında azalma gerektiren, enerji tüketiminde azalmaya yol açan ürünlerin üretimi için çok önemli özelliklere sahiptir. Bununla birlikte, kullanımlarının genişlemesini en çok sınırlayan şey, korozyon ve aşınmaya karşı zayıf direncidir. Bu, araştırmacıların dikkatini bu soruna bir çözüm bulmaya odaklamıştır. Araştırmacılar tarafından benimsenen çözümlerden biri kaplamadır ve magnezyum alaşımının kaplanmasında kullanılan tekniklerden biri de mikro ark oksidasyon kaplamasıdır ve bu projede AZ31 Mg alaşımının kaplaması esas alınacaktır. Bu alaşım yaygın olarak üretilmekte ve çok çeşitli kullanımlara sahiptir. Bu tezde, AZ31 alaşımının MAO kaplamasına TiO_2, TiN, TiC eklenmesinin etkisi çalışılacaktır.

Bu çalışma, AZ31 alaşımının MAO kaplamasına TiO_2, TiN, TiC ilavesinin etkisi üzerine yapılan ilk çalışmadır. Bu nedenle, bu bileşikler elektrolit çözeltisine eklenmiş

ve MAO teknolojisi ile alaşımın korozyon ve aşınmaya karşı direncini iyileştirme üzerindeki etkileri incelenmiştir. Kaplamadan sonra yüzey karakterizasyon incelemesi yapmak için SEM, XRD, XPS, FTIR, Raman analizleri gerçekleştirilmiştir. Elektrokimyasal korozyon deneyleri (elektrokimyasal empedans ve potansiyodinamik) ile kaplamanın korozyon özellikleri incelenmiştir. Bu tezde, MAO teknolojisinde TiO_2, TiN, TiC ekleyerek AZ31 alaşımının korozyon ve aşınma direncini önemli ölçüde artırmayı hedeflemektedir. Çalışmanın sonuçlandırılması ve ulaşılacak sonuçların yanı sıra magnezyum alaşımlarının kullanım alanları da artacaktır. Bu tez, aynı alanda araştırmacılar ve yeni bilimsel makaleler için bir veri tabanı sağlanmasına katkıda bulunacaktır.

Anahtar Kelimeler : Mikro ark oksidasyon, AZ31 alaşımı, korozyon, aşınma

Bilim Kodu : 91510

ACKNOWLEDGMENT

I would like to convey my gratitude to my esteemed supervisor, Assoc. Prof. Dr. Fatih AYDIN, who played the most important role in assisting me in the preparation, research, and coordination of this thesis and from whose experience and knowledge I benefited in working on the scientific foundations that led to the thesis' completion. I'd also like to express my gratitude to all of the personnel and supervisors at Karabuk University Iron and Steel Institute for their support throughout the laboratory testing.

I'd like to express my gratitude to the KBU-BAP unit for their support of this study, which was funded by the Karabuk University Scientific Research Projects Coordinatorship under the project number KBÜBAP-21-YL-087.

My heartfelt thanks to my family for their unwavering support and encouragement as I worked on my master's thesis.

I would also want to express my thanks and appreciation to my native country, Libya, which was represented by the Cultural Attaché at the Libyan Embassy in the Republic of Turkey, who assisted me and followed up with me.

CONTENTS

Page

Page

Page

LIST OF FIGURES

Page

Page

LIST OF TABLES

Page

SYMBOLS AND ABBREVITIONS INDEX

SYMBOLS

Al	: Aluminum
Al_2O_3	: Aluminum oxide
$C_3H_8O_3$	: Glycerin
Cr	: Chrome
Fe	: Iron
GO	: Graphene oxide
$KCl•MgCl_2•6H_2O$	: Carnallite
KOH	: Potassium hydroxide
$Mg(OH)_2$	: Magnesium hydroxide
Mg	: Magnesium
Mg_2SiO_4	: Forsterite
$MgCO_3$	: Magnesite
$MgCO_3•CaCO_3$	: Dolomite
$NaPO_3$	: Sodium metaphosphates
Si_3N_4	: Silicon nitride
SiO_2	: Silicon dioxide
Ti	: Titanium
TiC	: Titanium carbide
TiN	: Titanium nitride
TiO_2	: Titanium dioxide
$Zr O_2$	: Zirconium dioxide

ABBREVIATIONS

MAO	: Micro Arc Oxidation
ASTM	: American Society for Testing and Materials
UNS	: Standard Numbering System
SEM	: Scanning Electron Microscope
EDX	: Energy Dispersive X-ray Spectroscopy
XRD	: X-ray Diffractometry
FTIR	: Fourier Transform Infrared Spectroscopy

PART 1

INTRODUCTION

Due to mankind's urgent need to preserve the environment and reduce all the nefarious harms in this area on the one hand and on the other hand saving energy and cost, researchers seek to use metals with good mechanical specifications and low density, so there has been a high concentration of Mg, especially in the automobile and aircraft industries. Mg is a low-density metal with high specific strength and strong vibration damping properties. But one of its main drawbacks, which limits the expansion of its uses, is its weak resistance to wear and corrosion.

To reduce this defect, metal surface treatment techniques are used, such as micro arc oxidation, chemical / physical vapour deposition, thermal spraying methods, sol-gel, electrolytic deposition and among these techniques is the micro arc oxidation (MAO) which is also known as plasma electrolytic oxidation (PEO). MAO is commonly used for coating Ti, Mg, and Al alloys due to its benefits, such as low environmental impact and strong coating adherence to the metal, as well as the ease and variety of ways to regulate coating parameters. The coating process is carried out in the technique of MAO through the formation of a small electric arc on the surface of the alloy; due to the high electrical potential difference between the anode, which is the alloy and the cathode, an electric arc forms on the surface, causing partial melting and the creation of a coating layer on the alloy's surface, which enhances corrosion resistance.

Several factors influence the coating's quality, including voltage, the density of the electric current, electrolyte composition, process duration, and current type. The porosity of the coating is the main disadvantage of this method, as it reduces the effectiveness of the coating to resist corrosion. The most prominent solution used in recent years to overcome this defect is to add particles to the electrolyte by means

these additives, the thickness, density, and phase composition of the coating layer are changed.

When the previous literature was searched, it was found that a limited number of studies dealt with the effect of adding Ti compounds to the electrolyte in MAO technology. Previous studies in the literature have concluded that adding Ti compounds to the electrolyte solution when coating a Mg alloy with MAO improves the mechanical properties and enhances the corrosion and wear resistance, and this makes the uses of Mg alloys in various industries expand.

In this thesis, the effect of adding three Ti compounds (TiO_2, TiN, TiC), on the properties of AZ31 alloy, which is used in many industries, was examined using the MAO, so Ti compounds were added to the electrolyte solution in different percent (3, 6) g/l and then the effect on the coating surface was studied using by (SEM), X-ray diffractometry (XRD), Raman spectroscopy, and Fourier transform infrared spectroscopy (FTIR), the wear resistance of the coating was tested using (2, 4, and 6) N, and the corrosion properties of the coating were checked using electrochemical corrosion experiments.

PART 2

MAGNESIUM AND ITS ALLOYS

The proportion of Mg in the earth's crust is 2.7% and is extracted from sea water in an economical way and with a high degree of purity [1, 2]. Mg has attracted researchers and manufacturers, particularly in the cars, electronics, and aviation industries, as well as in medical and military industries, because of its characteristic density, which is equivalent to 1/4 of the density of Fe and two-thirds of the density of Al [2-7]. Among the most famous compounds in nature are Dolomite ($MgCO_3$•$CaCO_3$), Magnesite ($MgCO_3$), and Carnallite (KCl•$MgCl_2$•$6H_2O$). It is also found in large quantities in sea water, which makes its reserves very large. Mg is characterized by its low density of 1.738 g/cm^3 as compared with the density of some common structural alloys such as Al alloys (2.8 g/ cm^3), Die cast alloys of Zinc (6.6 g/cm^3), Cast iron (7.2 g/cm^3), and Ti (4.5 g/cm^3) [5].

2.1. PROPERTIES OF MAGNESIUM

2.1.1. Chemical Properties

From the handbook: magnesium and magnesium alloys [7] we have summarized some of the properties of magnesium which we show in Table 2.1.

Table 2.1. Magnesium properties [7].

Symbol	Mg	Crystal structure	Hexagonal closed pack (HCP)
Atomic Volume	14.0 cm^3/mol	Orbital electron configuration in free atoms	$1s^2,2s^2,2p^6,3s^2$

Atomic Weight	24.3050	Boiling point	1090˚C
Atomic Radius	0.160nm	Thermal conductivity (at 27˚C)	156 $W \cdot m^{-1} K^{-1}$
Density (at 20˚C)	1.738 g / cm^3	Specific heat capacity (at 20˚C)	1.025 $kJ\ kg^{-1} K^{-1}$
Most common valence	2+	Electrical conductivity	38.6% IACS

2.1.2. Mechanical Properties of Magnesium

Good ductility, higher damping qualities than Al, and excellent castability are some of the advantages of Mg. In addition, it is the lightest metal used and its good properties that make it the subject of research interest. Table 2.2 shows the mechanical properties of pure Mg at 20 °C.

Table 2.2. Mechanical properties of pure Mg at 20°C [7].

Form and section / Property		Extrusion	Sand cast	Hard rolled sheet	Annealed sheet
Tensile strength (MPa)		165-205	90	180-220	160-195
0.2% Tensile yield strength (MPa)		69-105	21	115-140	90-105
0.2% Compressive yield strength (MPa)		34-55	21	105-115	69-83
Elongation in 50 mm		5-8	2-6	2-10	3-15
Hardness	HRE	26	16	48-54	37-39
	HB	35	30	45-47	40-41

2.2. APPLICATIONS OF MAGNESIUM ALLOY

2.2.1. Applications in Aerospace

The aircraft industry always needs to search for a lower weight to reduce operating and fuel consumption costs and emissions [8, 9]. In the past, Al alloys were used, as

well as sheets of metallic fires and low-density structural plastics, and because of the limitations of the development that occurred in Al alloys for the purpose of reducing their weight and also because of the high cost of producing metallic fibre sheets, also with a decrease in some required properties, such as bearing shocks and temperatures. It was found that Mg is a good alternative in the aviation industry because it has a not high density with good mechanical properties[10]. For several years, Mg alloys have been used in many parts of civil and military aircraft due to their appropriate properties in terms of strength, low density, ease of manufacture, and the ability of Mg alloys to withstand high temperatures and bombardment of small meteorites and high-energy particles. Mg alloys were used to make Rockets and Spacecraft [10, 11].

2.2.2. Automotive Applications

One of the first car manufacturers to use Mg was Volkswagen. Then, in 1928, Bosch used an engine made of Mg [10]. One of the major motives that made designers and manufacturers interested in using Mg increasingly in the automotive industry is the urgent need to produce lighter cars to save fuel and reduce heat emissions, as reducing weight by 100 kilograms results in a fuel reduction of 0.5 liters per 100 kilometers the car travels. By combining the increased use of lighter materials with innovative designs for the automotive industry, cars that are lighter, less environmentally harmful and more fuel efficient can be achieved [10]. Figure 2.1 shows some Mg parts for cars [12].

Figure 2.1. Mg auto parts [13].

2.2.3. Medical Applications

There are many things that make Mg of interest to researchers for its use in the human body, including that the human body naturally contains Mg, approximately one mole of an adult weighing 70 kg. It is one of the components of the human body [11]. The elements used in the medical industries are always of a density similar to the density of human bones, and Mg has this feature [13] and one of the results of its previous uses in the human body was that its low corrosion resistance caused H to accumulate around the parts that were implanted in the human body, and this limited its uses in the human body. However, studies are continuing to overcome the weakness of corrosion resistance, including the use of various coatings of Mg alloys. In other words, Mg is among the medical uses after overcoming the weak corrosion by appropriate coating techniques [11, 13].

2.2.4. Electronic Applications

Also, here we find that the materials that are desirable when making electronic equipment are, in most cases, light in weight, easy to carry and durable. These specifications may be shared by Mg and plastic, but Mg is distinguished over plastic here in its ability to conduct and transfer heat as well as prevent radio frequency interference and electromagnetic wave interference [14]. Therefore, Mg alloys are employed for the production of mobile phone cases, laptops, and desktop computers. Also, Mg alloys are employed for the manufacture of hard disk drive shafts and heat sinks due to their heat dissipation properties and the possibility of forming them to produce complex shapes [14].

2.2.5. Sports Applications

Each industry has needs and specifications that determine the path of researchers and designers. Sports equipment must be appropriate for the purpose for which it will be used. It requires lightness in weight and appropriateness in shape due to the low density of Mg alloy and the ease of producing complex shapes used in the manufacture of some sports equipment, such as the handles of table tennis racquets. The golf club also

used Mg alloy in the manufacture of the frame of inline skates and bicycle tires because it has properties such as absorbing shocks and vibrations [10, 14].

2.2.6. Other Applications

Due to its light weight, Mg was also employed in the construction of eyeglass frames, as well as equipment such as rifle scopes and binoculars that benefited from light weight and optical stability. In order to obtain higher efficiency in manual work equipment and to make the equipment lighter, Mg alloy was used to make handles for manual scissors, household drilling machines, and household equipment gears [10].

2.3. MAGNESIUM ALLOYS

Metal alloys are metals to which another element or several elements have been added, and this occurs for the purpose of modifying the properties of the metal to enhance a specific property. Sometimes the alloy consists of adding several elements to a metal or more than one metal. For example, Cr alloyed with steel to improve corrosion resistance of the steel and so on. Alloys are created to avoid a specific defect when the metal is used or to enhance certain specifications [15].

2.3.1. Effects of Adding Alloying Elements to Mg alloys

To overcome the deficiency of Mg in terms of some mechanical properties, many elements must be mixed with pure Mg to produce Mg alloys with the necessary mechanical properties. The effect of these elements on the corrosion resistance and mechanical properties can be observed. Significant progress has been made in the strengthening of Mg alloys by solid solution strengthening with various alloying components [16]. During the following points, the effect of adding some elements to magnesium alloys was discussed.

2.3.1.1. Aluminum

Adding Al to Mg improves strength, hardness, and makes casting the alloy easier, which prolongs the freezing process. The alloy is more amenable to heat treatment when the percentage of Al is greater than 6% by weight, which is usually not more than 10% by weight. Therefore, Al is the most suitable element for Mg alloys compared to the rest of the other elements [7, 16].

2.3.1.2. Zinc

Zn is frequently added to Mg alloys to improve their strength at room temperature. When zinc is added to Mg alloys having 7 to 10% Al, at a percentage greater than 1%, the heat shortness of the alloy is increased. When a mixture of Zn is added with Zr, Th, or rare earths, an alloy of Mg has good strength and is difficult to precipitate. Also, if Fe and Ni impurities are present in the Mg alloy, adding Zn to it helps to overcome their corrosive impact [7, 16]. When Zn is added to Mg alloys in sufficient quantities, it improves the strength and does not reduce the ductility [17].

2.3.1.3. Manganese

Even though Mn does not improve the tensile strength of the Mg alloy, it does raise the yield strength slightly. The addition of Mn to Mg alloys has the most significant effect on the resistance of saltwater of Mg-Al-Zn and Mg-Al alloys [7].

2.3.1.4. Zirconium

When Zr is added to Mg alloys, it acts as a powerful purifier for the grains in the alloy. The addition of Zr to the alloy contributes to improving the mechanical properties at ambient temperature, the corrosion performance of the alloy, and the ability to cast, through its contribution to obtaining a fine granular structure [17]. When Zr is added to a Mg alloy, including components like Fe, Mg, C, Si, and O, it produces compounds with any of these elements and is stable compound and, as such, is eliminated from the solid solution [7].

2.3.1.5. Rare earth elements

When an element of rare earth is added to Mg alloys, they increase the strength of the alloy at clavated temperatures. It also reduces the porosity when casting as it narrows the casting range [7].

2.3.2. AZ31 Alloy

Mg alloy, which is known by the symbol AZ31, which is the alloy on which we conduct our study, is an element of Mg, to which Al and Zn are added as two main elements in the alloy with the rest of the elements in proportions as follows: Al (2.5-3.5 wt%), Zn (0.6-1.4 wt%), Mn (0.2-1.0 wt%), Si (0.08 wt%), Cu (0.01 wt%), Ni (0.001 wt%), Fe (0.003 wt%). Adding the element Al to the alloy improves its hardness and strength, as well as its castability [18, 19]. According to the ASTM, the Mg alloy AZ31 is produced by the forging technique. M11311 is the Unified Numbering System (UNS) code for the AZ31 alloy [16]. Table 2.3 gives some of the mechanical properties of AZ31 [14].

Table 2.3. Yield, tensile strength and ductility of AZ31 alloy.

	Ductility, % at 50mm	Yield Strength, MPa	Tensile Strength, MPa
AZ31	15	200	262

Many industries use Mg alloys, like the automobile and transportation industries, as well as the medical industries, because of their special properties such as high strength, density is not high, dimension stability, high specific energy, and cutting machining performance and have thus gained prominence. While this is of interest to many researchers, it is fair that some defects limit the use of Mg alloys, such as poor resistance to wear and corrosion [20].

2.4. CORROSION AND WEAR BEHAVIORS OF Mg ALLOYS

Due to the many advantages that Mg and its alloys have in mechanical properties, the cheapness of its production cost, the fact that it is available in abundance and can be extracted from sea water, as well as its being environmentally friendly, especially in

terms of its light weight and lower energy consumption, researchers are increasingly interested in finding ways to overcome its most prominent shortcomings, which are its weak resistance to corrosion and wear [1, 2, 4, 5]. This chapter covers the corrosion types of Mg alloys, the most important parameters affecting wear and corrosion behaviours, and methods of corrosion treatment.

2.4.1. Corrosion Behavior

The corrosion resistance of Mg alloys under normal environmental conditions is comparable to or even better than that of mild steel [10], and most of the time, the reasons for poor corrosion resistance are poor design, surface contamination, the presence of impurities, galvanic pairs, or inappropriate or insufficient surface protection methods [21, 22]. Because of the polarization caused by the formation of a thin layer of $Mg(OH)_2$, the corrosion potential of Mg at room temperature is slightly more negative than 1.5 V, and it is placed in a neutral solution or dilute chloride for the H electrode, despite the fact that the standard electrode potential of Mg is at -1.5 V. The room temperature is -2.37 V. Magnesium oxide formed on the surface of the metal provides surface protection in some environments, and the corrosion rate is between the corrosion rate of low carbon steel and the corrosion rate of Al [21]. Ions of sulfate, chloride, nitrate and several other ions formed lead to the destruction of the passivity of Mg. The protective film formed on the metal is broken by the chlorides, even if their quantities are small [21].

The most common types of corrosion in Mg alloys [10] are:

- Pitting corrosion
- High temperature corrosion
- Intergranular corrosion
- Stress corrosion
- Galvanic corrosion

2.4.2. Wear Behavior

When the main metal comes into contact with another metal, the gradual and continuous loss of material on the surface of the metal is known as wear [23]. Different

wear mechanisms occur for Mg according to the load and speed to which the metal is exposed. To overcome the shortcomings in some properties, including wear resistance in pure Mg, scientists recently focused on Mg metal matrix compounds (Mg-MMCs) as potential alternatives for the aerospace, automobile and military industries [3, 24]. The wear mechanism of magnesium alloys (adhesion, scuffing, abrasion or oxidation) is either physical or chemical [25-27]. The pattern of wear and its behaviour depends on the materials that make up the sample as well as the materials that make up the surface with which the sample comes into contact, in addition to other factors such as the speed with which the slip is carried out and the amount of load applied to the sample. Poor wear resistance limits the use of Mg alloys [25]. Alloy surface modifications by coating techniques are one effective way to overcome this problem [28].

2.5. WAYS TO REDUCE CORROSION

Several techniques are used to reduce the corrosion process of Mg alloys. One of the ways to reduce corrosion in Mg is the formation and production of alloys, which leads to the formation of second-phase precipitates. Mechanical and thermal treatments are performed to refine the granular structure and to control the distribution and quantity of the second-phase precipitates [2, 29]. Surface modifications are one of the techniques used to reduce the rate of corrosion of Mg alloys by forming a protective layer of ceramic, polymer, or composite [30-34], which does not change the structure of the alloy and thus effectively preserves the mechanical properties. Among the methods used to overcome the problem of corrosion of Mg alloys are electrochemical deposition [30], chemical conversion [31], organic coating [32], and micro-arc oxidation (MAO) [33]. Due to its strong adhesion and good resistance to corrosion and wear, MAO technology has gained the attention of many in recent years. It was found that in order to solve the problem caused by the pores formed in the coating layer, an additional sealing treatment is required, and it was noted that adjusting the electrolyte composition and changing electrical parameters only reduces the porosity and is not enough to close it [34-36]. An additive must be added to the electrolyte solution to close the pores [2, 37].

PART 3

MICRO ARC OXIDATION TECHNIQUE

3.1. MAO: ITS EVOLUTION AND HOW IT WORKS

The MAO process is a method of forming protective coatings on the surface of an electrically conductive metal alloy. This metal is immersed in electrolyte, and a high voltage is used to ensure the creation of a micro-arc discharge that moves across the metal's surface via anodic polarization [38]. Two American scientists, W. McNeil and L. Gruss, established the viability of employing anode sparks to generate a layer of oxides from alloy and electrolyte components in the early 1950s and 1960s. This was the start of the (MAO) technique's research [39], when the research of Russian scientist Markov, the discovery's originator, was published, this approach was widely used in Russia and around the world. Several advantages appear for this technique compared to other methods of creating coatings on the surfaces of light metals.

MAO technology is an alloy surface treatment method that produces an inorganic ceramic coating used for light metal alloys like Ti, Al, and Mg [40, 41]. One of the most prominent features of the MAO technology is that it produces a coating with superior mechanical properties such as metal substrate adhesion, hardness, and fatigue resistance, as well as chemical and physical properties such as heat protection, breakdown voltage, and thermal shock resistance. It is also characterized by being less expensive as it saves time and procedures because it does not require degreasing the surface of the alloy, washing, or clarification. It is environmentally friendly as it uses aqueous solutions with relatively small and non-toxic chemical components [38]. MAO process is the process of producing a ceramic coating on the surface of light alloys like Mg, Al, Ti, and Zr. This coating is formed through high-voltage anodic deposition [39].

The components of this system are an electrolyte bath, cathode, anode, power supply, and cooling system [40]. The technique of MAO has been developed and taken care of in recent years. In this process, the alloy to be coated represents the anode, and the cathode is chosen from a material that does not dissolve in the electrolyte solution. It produces oxides for the components that make up the alloy surface. The high breakdown voltage induces the production of a ceramic coating with a high porosity of oxides. The electrolyte is constantly stirred to ensure continuity of homogeneity, and the solution is cooled so that its temperature does not rise. By adding certain chemicals to the electrolyte, the coating quality can be increased. Some additive compounds improve corrosion resistance, and some improve the homogeneity and resistance of the coating [20, 41, 42]. Figure 3.1 shows the components of the coating process used in MAO process.

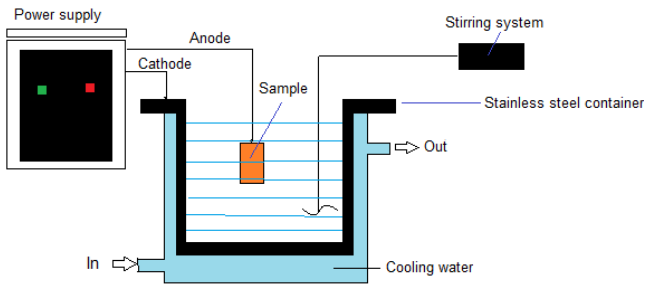

Figure 3.1. The schematic view of the MAO system.

3.2. MAO'S ADVANTAGES AND DISADVANTAGES

One of the benefits of MAO technology is that it creates a relatively thick coating on the surface of the alloy, which improves hardness, dielectric strength, thermal resistance, coefficient of friction, as well as corrosion and wear resistance, and the coating process can be completed during a reasonable amount of time. It can also create a homogeneous coating on irregular surfaces [43]. Providing corrosion resistance while not polluting the environment [38]. This method also produces a covering with excellent adherence to the alloy [44]. The MAO coating technique has both advantages and disadvantages. One of the disadvantages is that applying the coating to large components is extremely expensive due to the high voltage and current employed. The

second is that when a high electric field is applied, dielectric breakdown occurs in the oxide layer created on the alloy's surface, lowering energy efficiency and increasing energy consumption [45]. Another disadvantage is the high porosity of the resulting weld layer. However, this defect can be solved by using techniques such as adding particles of compounds to the electrolyte that minimize porosity [46].

3.3. PARAMETERS AFFECTING THE QUALITY OF MAO COATING

Electrolyte composition and electrical parameters have a substantial effect on the growth characteristics, microstructure, and phase composition of MAO-coated Mg alloys, which in turn has an impact on resistance to corrosion. In addition, the corrosion behaviour is affected by the phases of the coating layer, which can be controlled by adding insoluble compounds to the electrolyte. The composition of the Mg substrate also affects the phases of the coating layer [37, 47].

3.3.1. Electrical Parameters

Because the MAO coating process is an electrochemical and thermal oxidation process that is also influenced by micro discharge, the voltage and electric current density, as well as the duration of the current application, are the main electrical factors that influence the coating process and its properties [46].

3.3.2. Electrolyte Content

One of the important parameters which have a big role on the structural characteristics of the MAO coatings, such as porosity, shape, dispersion, formation processes of coating, the composition of coating, and final corrosion resistance, is the electrolyte composition. Aluminates, phosphates, and silicates are some of the electrolytes often utilized in MAO coatings [46-48]. For MAO coatings of Mg alloys, alkaline electrolytes are commonly utilized. In MAO, alkali metal hydroxides (such as Potassium hydroxide (KOH) are frequently utilized to modify the pH of the electrolyte composition. In addition, these chemicals improve the conductivity of the MAO solution, which changes the pH [42]. The higher the conductivity of the solution, the

thinner the coatings and the greater their porosity. KOH is an effective compound for lowering electrolyte conductivity [47]. When comparing the effects of using sodium silicate and sodium phosphate as an electrolyte mentioned in a study conducted by K. Rama et, al. [46], it was found that:

The coatings formed in the phosphate electrolyte

- Have more micropores.
- Is composed of MgO phase.
- The corrosion current density of the coating is 12 times lower than that of bare AM60B Mg alloy.
- The formation of coatings is faster.

The coating formed in the silicate electrolyte

- Is compact and uniform.
- Is composed of MgO and Mg_2SiO_4 phases.
- The corrosion current density of the coating is 55 times lower than that of bare AM60B Mg alloy.
- The coatings produced is harder.
- Better adhesion strength and wear resistance.

Increasing the concentration of $NaPO_3$ phosphate beyond above 5 g/l in the electrolyte leads to the formation of large porosity and increases the surface roughness, which leads to a decrease in corrosion resistance [49]. When comparing the electrolyte containing potassium ions with another containing sodium ions, the coating formed is more corrosion resistant [50]. The thickness and nature of the layer formed on the surface of the alloy using MAO technology is affected by the composition and concentration of the electrolyte used in the coating process [51].

3.3.3. Particle Addition

Changing the electrolyte composition is another technique to enhance coating quality by optimizing the morphology and composition. Recently, studies have been conducted on the addition of nanoparticles to the solution used in the MAO coating process to improve the thickness and compactness of the layer. Due to changes in pH, conductivity, and viscosity in the electrolyte composition, particle addition has an effect on the MAO process. Ag, MoS_2, SiO_2, Al_2O_3, CeO_2, and graphite are particle reinforcements commonly employed in MAO coatings to give lubricating qualities, chemical resistance and stability, increase antibacterial properties, and allow for high hardness [52]. Table 3.1 lists the particles used in the literature for several Mg alloys and their effects on the coating characteristics.

Table 3.1. The effect of nanoparticle addition on MAO coating characteristics.

Particles	Base Material	Results
Al_2O_3	AZ31	Corrosion improvement by pore filling and coating homogeneity improvement [47].
TiO_2	Mg-1%Ca	Corrosion decreases with the application of a hydrophobic coating and the filling of pores [47].
Si_3N_4	AZ31	Corrosion resistance is improved by depositing a new Mg_3SiO_4 phase and thickening the protective layer [47].
Graphene oxide	AZ31	Corrosion resistance is improved by forming a compacted morphology [47].
ZrO_2	AZ91	The coatings were given substantial anti-corrosion stability by blocking the pores at low concentrations. Due to the production of amorphous phases in coatings, raising the concentration up to 2 g/L has a detrimental impact [53].
SiO_2	AM50	Particle additions increase the wear resistance of PEO coatings, although corrosion resistance is marginally lowered, according to the findings [54].
$C_3H_8O_3$	AZ91D	Addition of $C_3H_8O_3$ to the electrolyte when coating AZ91D alloy resulted:- Coating thickness decreases, Reduces the number and size of pores, and Improves the corrosion resistance of the alloy [55].
Nano-SiC	AZ91D	Resulted from adding nano-SiC to the electrolyte when coating AZ91D alloy:- The porosity of the coating decreases and its density increases, the thickness and hardness of the coating increases, the coefficient of friction decreases, the wear rate decreases, and the corrosion resistance is improved [56].

8-HQ	AZ91	Due to the addition of 8-Hydroxyquinoline (8-HQ) to the electrolyte when coating AZ91 alloy: - Color change, pore size reduction, and corrosion resistance improvement [57].

PART 4

TITANIUM CARBIDE, TITANIUM NITRIDE, TITANIUM OXIDE

4.1. TITANIUM CARBIDE

TiC is a refractory ceramic substance that is exceptionally hard (9–9.5 Mohs) and, making it equivalent to tungsten carbide. Its appearance is a black powder and has a sodium chloride crystal structure (face-centered cubic). Its crystals size ranges from 0.1-0.3 mm in size as seen in nature. It's a form of the extremely uncommon mineral khamrabaevite that may be found in nature. It was discovered in 1984 near the Uzbek border on Mount Arashan in the Chatkal District, USSR (now Kyrgyzstan) [58, 59].

4.1.1. Properties of TiC

TiC carbide has 188 GPa shear modulus and 400 GPa elastic modulus. The following Table shows some properties of titanium carbide [58, 59].

Table 4.1. Some properties of TiC [58, 59]

Chemical symbol	TiC
Appearance	Black powder
Mass	59.89 g/mol
Density	4.93 g/cm^3
Melting point	3,160 °C
Boiling point	4,820 °C
Solubility in water	It does not dissolve in water
Magnetization property	$+8.0 \cdot 10^{-6}$ cm^3/mol
Hardness	28 – 35 GPa

4.1.2. Applications of TiC

TiC is used to make cermites, which are widely used for mill materials at high cutting speeds. It is also used as a wear-resistant coating on parts used on metal items like tool bits and watch [60]. TiC is also employed as a heat barrier during spacecraft reentry into the atmosphere [61].

4.2. TITANIUM NITRIDE

TiN which is also called Tinite is an exceptionally hard ceramic substance that is commonly used to enhance the surface qualities of titanium alloys, steel, carbide, and aluminum components. TiN is employed as a protective coating for hardening sliding surfaces. It is also used for cosmetic purposes because TiN looks golden, and it is used for medical purposes because it is not toxic as an outer layer for manufactured parts. A covering of less than 5 micrometers is used in most applications, one of the advantages of TiN coating is its biocompatibility with good mechanical properties [62].

4.2.1. Properties of TiN

The hardness of TiN ranges from 1800 to 2100 HV, a 251 GPa elastic modulus, a 9.35106 K1 thermal expansion coefficient, and a 5.6 K superconducting transition temperature [63]. When using TiN in ionic paint for use in decorations, and then testing the paint's resistance to scratching, it gave better results than paint made of stainless steel [64]. When coating titanium alloy with titanium nitride using coating PVD technique it was found that the corrosion resistance was significantly improved [63]. TiN has (0.4-0.9) a friction coefficient against another TiN surface, depending on the substrate material and surface polish. The usual TiN formation has a NaCl-type crystal structure with a stoichiometry of about 1:1[63]. The following table shows some properties of TiN.

Table 4.2. Some properties of TiN [63].

Chemical symbol	TiN
Appearance	Appears in gold when coated with it
Mass	61.874 g/mol
Density	5.21 g/cm^3
Melting point	2,947 °C
Solubility in water	Insoluble
Magnetization property	$+38\times10^{-6}$ emu/mol
Hardness	18-21 GPa

4.2.2. Applications of TiN

TiN is used in the manufacture of drill bits and parts of machinery requiring high resistance to abrasion and wear. These are well-known applications for TiN coating, which may increase the number of times it is used [65]. Also, from the use of TiN in painting things for the purpose of decoration, such as some ornaments and jewelry, as well as car parts because of its metallic gold color. It's utilized as a coating in In the fields of military manufacturing and equipment in the field of space, as well as to protect the surfaces of bicycle and motorcycle [62]. The addition of TiN nanoparticles to the MAO-coating increases the mechanical properties of the surface of Mg alloys substantially. As a result, the scope of use for these materials may be expanded in industries including aerospace, automotive, and the production of high-tech products and equipment [66].

4.3. TITANIUM DIOXIDE

It’s a chemical substance having the formula TiO_2. It is sometimes called white titanium and is used in dyeing. Although mineral forms might seem black, it is a white, water-insoluble solid. Paint, sunscreen, and food coloring are just a few of the applications for this pigment [67]. TiO_2 is an oxide substance that is chemically stable, ecologically friendly, and functionally flexible. Nano - crystalline Ti uncovers applications in a variety of emerging fields, such as paints, coatings, papers and inks,

and medical equipment coated with Ti nanofilms in addition to regular applications such as pigment, metallurgy, and catalysis applications [63].

4.3.1. Properties of TiO_2

Titanium dioxide has several properties that distinguish it for use in many uses, as its melting temperature is 1843 degrees Celsius, while it boils at a temperature of 2972 °C, and therefore it is found in nature in a solid form, and it does not dissolve in water and because of the way it absorbs ultraviolet rays It looks pure white in appearance and has a great ability to scatter light, which makes it suitable for aesthetic uses [68].

4.3.2. Applications of TiO_2

As a surface coating, TiO_2 is frequently used. for ultraviolet rays' resistant qualities in plastics and other applications [69]. The MAO coating's thickness grew, and its color changed from light grey to dark grey. It was mentioned in a study of the effect of adding TiO_2 nanoparticles on the microstructure of a coating on a magnesium alloy AZ91 conducted by Song, Y. et al., that the addition of TiO_2 to the coatings might help to reduce the number of pores and increase the density of the coatings. The drop time rose as the corrosion current density decreased. The fact that TiO_2 nanoparticles may enhance the thickness and density of the coatings on the AZ91 magnesium alloys increased the corrosion resistance of the modified coatings [70].

In this study, we investigated the effect of TiO_2, TiN and TiC on the properties of the coating produced on the surface of AZ31 alloy when these compounds were added as nanoparticles to the electrolyte in the MAO process in order to improve the alloy. Corrosion and wear resistance. As there is enough information in the literature covering the investigation of the addition of TiO_2, TiN, TiC from MAO coating on AZ31 alloy properties, which will provide new data leading to the expansion of the uses of AZ31 alloy in industries.

PART 5

EXPERIMENTAL STUDIES

5.1. SAMPLE PREPARATION

The substrate material in this research was AZ31 alloy. The composition of the AZ31 alloy used in the study is shown in Table 5.1.

Table 5.1. Chemical composition of the AZ31 alloy used in the study.

Element	Al	Zn	Mn	Ca	Fe	Mg
%wt.	2.9	1.2	0.22	0.03	0.003	The rest

The samples were 50 x 10 x 5mm in size, and they were cut with precision cutting equipment (Figure 5.1) before being sanded with SiC sandpaper (between 240 and 2500 mesh) in a sanding-polishing machine (Figure 5.2). The samples were prepared for coating by being cleaned in alcohol and sanded before drying.

Figure 5.1. Precision cutting device.

Figure 5.2. Sanding-polishing device.

5.2. COATING PROCESS

For MAO operation, a DC power supply is utilized. Na_2SiO_3 (10 g/L), NaOH (6 g/L) were used as the basis electrolytes, with the samples for the study were divided as shown in Table 5.2, at distinct voltages, 225V, the coating voltage was investigated. All samples were coated for the same amount of time, which was 8 minutes. Table 5.2 lists the electrolytes and sample names, and (Figure 5.3) shows sample surface pictures before and after coating.

Table 5.2. Sample names and particle addition concentration.

Sample No.	Electrolytes	Particle addition (wt. %)	Name
1	Base solution	-	MAO
2	Base solution + TiO_2	(3 g/L)	MAO (TiO_2)
3	Base solution + TiO_2	(6 g/L)	MAO (TiO_2)
4	Base solution + TiN	(3 g/L)	MAO (TiN)
5	Base solution + TiN	(6 g/L)	MAO (TiN)
6	Base solution + TiC	(3 g/L)	MAO (TiC)
7	Base solution + TiC	(6 g/L)	MAO (TiC)

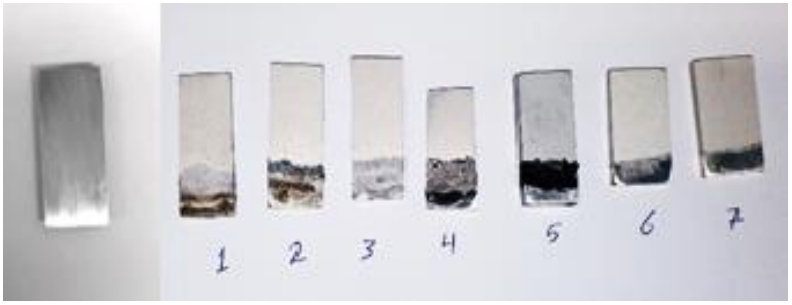

Figure 5.3. The uncoated and coated samples.

The pH of the electrolyte during coating is 12.5. The continuous stirring system during the coating process ensures that the nanoparticles added with the electrolyte are homogeneous throughout the coating period. As well as the cooling system makes the temperature of the solution does not exceed 35°C. The components of the coating equipment used in the coating process are shown in the (Figure 5.4).

Figure 5.4. Coating process equipment.

5.3. STUDIES THE COATING'S CARACTERIZATIONS

A Carl Zeiss Ultra Plus scanning electron microscope (SEM) equipped with EDX (Bruker) was used to study the coatings' surface and cross-sectional pictures (Figure 5.5). The coatings were analyzed using a Rigaku Ultima IV X-ray diffraction (XRD) system (Figure 5.6) and Fourier transform infrared spectroscopy (FTIR) (Figure 5.7). X-ray photoelectron spectroscopy (XPS) has also been used to identify the components of the coating. Raman spectroscopy used to obtain information on the composition and chemistry of surfaces and to identify existing materials.

Figure 5.5. Scanning electron microscope.

Figure 5.6. X-ray diffraction system.

Figure 5.7. FTIR device.

5.4. WEAR – ROUGHNESS TESTS

A reciprocating wear tester (UTS 10/20) was used to examine the samples' wear performance under loads of 2, 4, and 6N under dry sliding conditions conditions (Figure 5.8). 30 m was chosen as the sliding distance. A Profilometer was used to assess the surface roughness of the coated samples (Figure 5.9). After the wear tests, the coating surfaces were inspected using a scanning electron microscope (SEM).

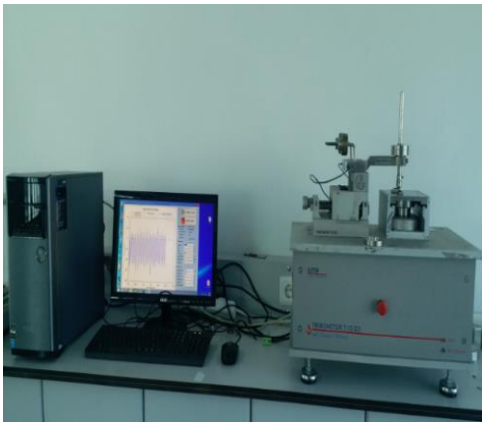

Figure 5.8. Reciprocating wear tester.

Figure 5.9. Profilometer device.

5.5. CORROSION TESTS

Potentiodynamic polarization and electrochemical impedance spectroscopy with a galvanostat (Partstat 4000) were used to analyze the samples' corrosion performance (Figure 5.10). A 3.5 wt.% NaCl solution was used to make the corrosive medium. Ag/AgCl and graphite, sequentially were used as the reference and counter electrodes. 1.5 mV/s was chosen as the scanning rate. EIS experiments were conducted at frequencies ranging from 100 kHz to 0.1Hz. The voltage signal's amplitude was fixed at 10 mV.

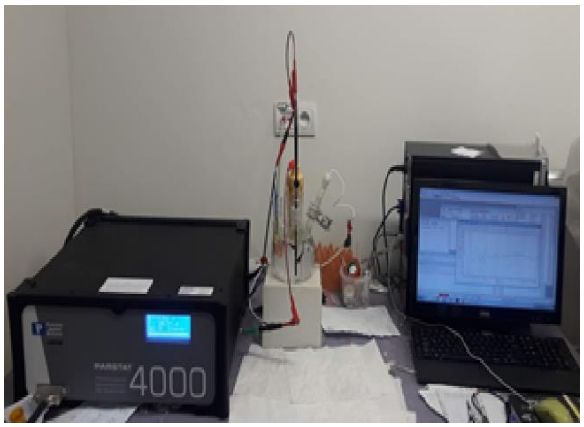

Figure 5.10. Corrosion test device.

PART 6

RESULTS AND DISCUSSION

6.1. COATING CHARACTERIZATION

Figure 6.1 and Figure 6.2 shows the surface images of the coatings for 3 g/l and 6 g/l, respectively. As can be seen from the figures, there are no microcracks on the coating surfaces, and there are crater-type pores. The presence of crater-type pores in MAO coatings is attributed to the ejection of molten oxide and gas bubbles from the MAO channels [71]. Several researchers have reported the presence of crater-type pore structure after MAO coating for Mg alloys [37, 54, 72]. It is seen from the figures that the maximum pore diameter is obtained in MAO coatings without nanoparticle addition. However, it was detected that the pore diameter decreased with the addition of nanoparticles to the MAO solution. For 3 g/l, the mean pore diameter was measured as 1.05 µm, 0.71 µm, 0.64 µm, and 0.51 µm for coatings MAO, MAO (TiN), MAO (TiO_2), and MAO (TiC), respectively. For 6 g/l, the mean pore diameter was measured as 1.05 µm, 0.86 µm, 0.79 µm, and 0.71µm for coatings MAO, MAO (TiN), MAO (TiO_2), and MAO(TiC), respectively. The high energy density in the electrolyte without nanoparticles results in larger discharge sparks and larger melt discharging channels. As a result, after the solidification of the melted products in the channels, larger pores remain on the surface and the pore size increases [73, 74]. For 3 g/l, the surface roughness (R_a) was measured as 0.19 µm, 0.18µm, 0.16µm and 0.15 µm for coatings MAO, MAO (TiN), MAO (TiO_2), and MAO (TiC), respectively. For 6 g/L, the surface roughness (R_a) was measured as 0.19 µm, 0.38 µm, 0.29 µm, and 0.26 µm for coatings MAO, MAO (TiN), MAO (TiO_2), and MAO (TiC), respectively. The reason for the increase in the surface roughness with the increase of the nanoparticle content is that the incorporation of nanoparticles in the coating pores during electrophoresis and therefore, the height of the peaks on the surface is greater than the depth of the voids [66]. Microstructure investigations showed that coatings with TiC

nanoparticles had the best sealing effect. This is associated with the individual characteristics of the micro-discharges and the preferred location of the particles in the pores [75]. As the nanoparticle content increases from 3g/l to 6 g/l, it is seen that some pores are partially filled with nanoparticles (Figure 6.2).

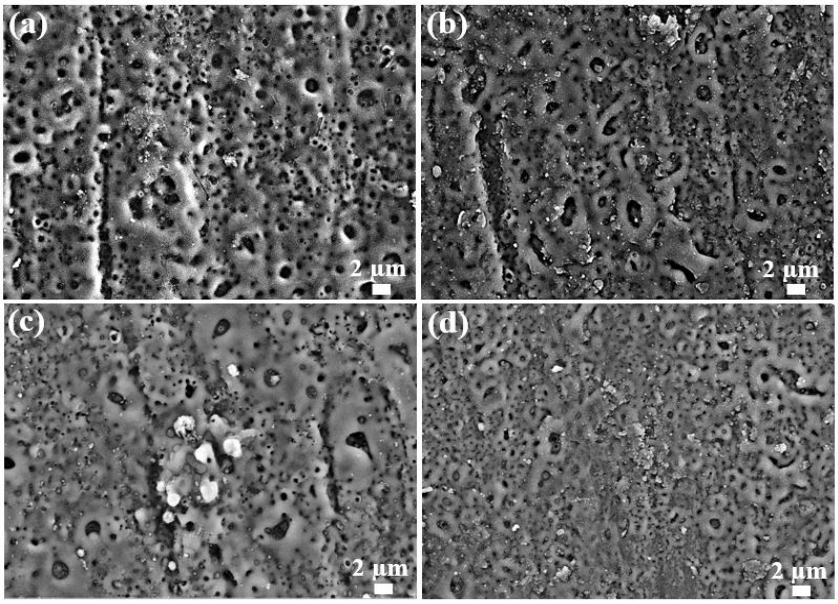

Figure 6.1. Surface morphologies of the coatings for 3 g/l: a) MAO, b) MAO(TiN), c)MAO (TiO2), and d) MAO (TiC).

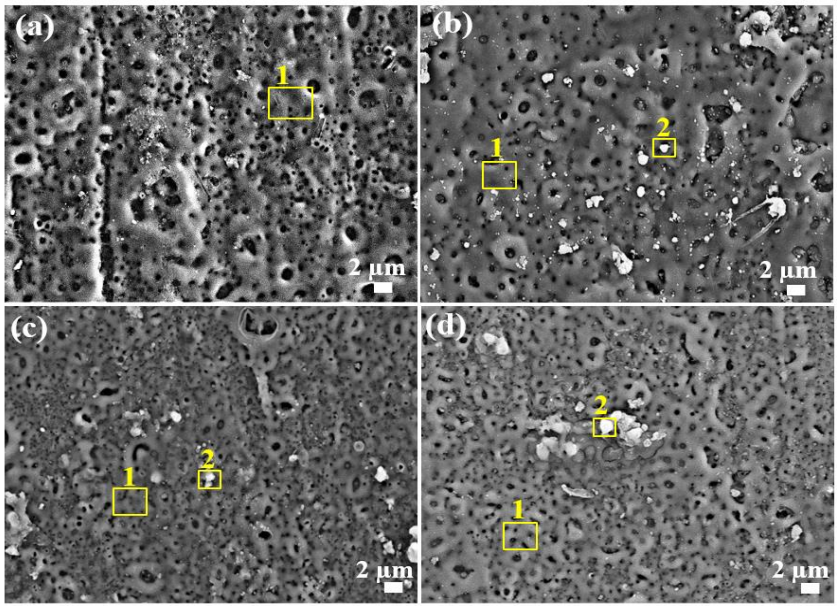

Figure 6.2. Surface morphologies of the coatings for 6 g/l: a) MAO, b) MAO(TiN), c)MAO (TiO2), and d) MAO (TiC).

EDS analyzes were taken from some regions of the coatings in Figure 6.2, and the results are given in Table 6.1. Analyzes with code 1 were taken from areas without particles. According to the results of analysis number 1 for all coatings, the presence of Mg, O and Si elements at high content in the structure was detected. For example, for the analysis of MAO-1, the content of Mg, Si and O was 23.59, 12.69, and 60.66, respectively. The presence of Mg, O and Si verifies the formation of MgO and Mg_2SiO_4 on the coating structures [6]. The low content of Na and Al comes from the electrolyte and substrate, respectively. For the analysis of MAO (TiN)-2, the high content of Ti (16.05%) is detected. This verifies the presence of the TiN nanoparticles on the coating surface. For the analysis of MAO (TiO_2)-2, the high content of Ti (11.27%) and O (72.80%) detection proves the presence of TiO_2 in the structure. For the analysis of MAO (TiC)-2, the Ti and C content was 15.43% and 15.62%, respectively. This proves the incorporation of TiC particles on the coating surface.

Table 6.1. EDS results of the different MAO coatings (6g/l).

Coating	O	Si	Mg	Na	Al	Pt	Ti	N	C
MAO-1	60.66	12.69	23.59	1.20	0.38	1.47	-	-	-
MAO (TiN) -1	58.78	13.77	22.76	0.94	0.07	2.39	1.30	-	-
MAO (TiN) -2	70.14	6.26	4.40	1.0	-	2.15	16.05	-	-
MAO (TiO_2)-1	58.43	11.23	27.14	1.93	0.02	1.25	-	-	-
MAO (TiO_2)-2	72.80	5.16	6.06	2.94	-	1.77	11.27	-	-
MAO (TiC)-1	56.71	10.98	24.15	0.76	0.42	1.87	-	-	5.11
MAO (TiC)-2	53.55	7.21	1.17	0.71	0.09	6.21	15.43	-	15.62

Figure 6.3 shows the cross-section images of the coatings with nano-particle addition. The maximum coating thickness was obtained for the MAO(TiC) coating. The coating thickness of the MAO(TiC), MAO(TiO_2), and MAO(TiN) was noted to be 6.2 µm, 4.7 µm, and 3,5 µm, respectively. From the cross-section images, dense structure and smooth surface are observed for the MAO(TiC) coating. The obtaining of different coating thicknesses by adding different nanoparticles was based on the change of the nature of the micro discharges due to the presence of particles in the electrolyte [75].

The result of the EDS analysis taken from the cross section of MAO (TiC) in Figure 6.3 is given in Table 6.2. The significant amount of Mg (48.04%) and O (23.75%) was detected. This verifies the presence of MgO in the cross-section of coating. The Ti and

C were also detected for the analysis. This is the result of the incorporation of TiC particles to coating structure.

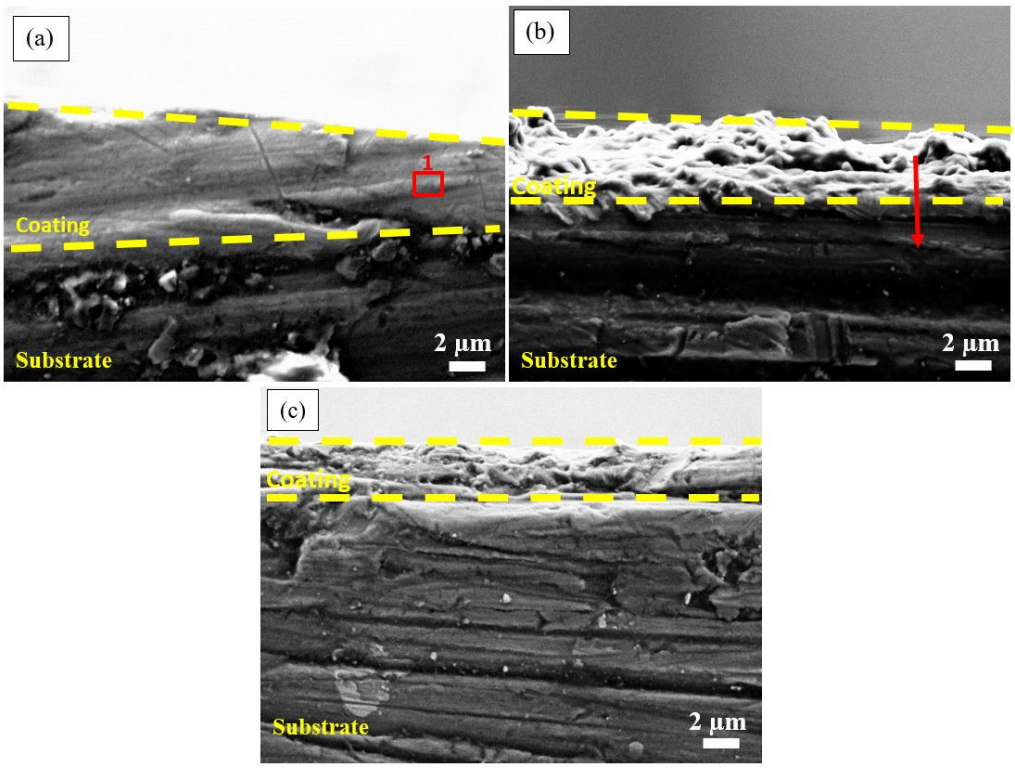

Figure 6.3. Cross-section images of the coatings a) MAO (TiC), b) MAO (TiO_2) and MAO(TiN).

Table 6.2. EDS results of the cross-section of MAO(TiC).

wt.%	O	Si	Mg	Zn	Al	Ti	C
1	23.75	2.61	48.04	1.83	1.15	9.11	13.51

Figure 6.4. shows the line EDS analysis of the MAO (TiO_2) coating (in Figure 6.3). For the coating area, the presence of high content of Mg, Si and O elements was proved for the coating area. The presence of a low amount of Ti is also seen. For the substrate area, the Mg content significantly increased. The content of other elements in the substrate region is very low.

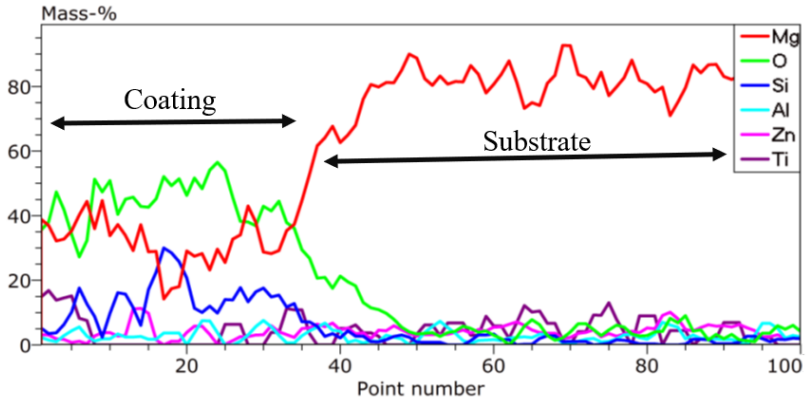

Figure 6.4. Line EDS analysis of the MAO (TiO2).

Figure 6.5 shows the XRD patterns of the coatings for 6 g/l. The presence of similar peaks was observed for all coatings. For XRD analysis, the MgO, Mg_2SiO_4 and Mg peaks were detected. The presence of Mg peaks is explained by the penetration of X-rays into the substrate due to the thin coating thickness [37]. It is also observed that the peak intensity of MgO is the highest. Aydin et al. reported the presence of MgO and Mg_2SiO_4 phases for MAO coating with silicate electrolyte [6]. For the XRD analysis of the coatings, no peaks were detected belonging to TiC, TiO_2 and TiN. This is because the nanoparticle content on the coating surface is very low, so it cannot be detected in standard XRD measurements [76, 77].

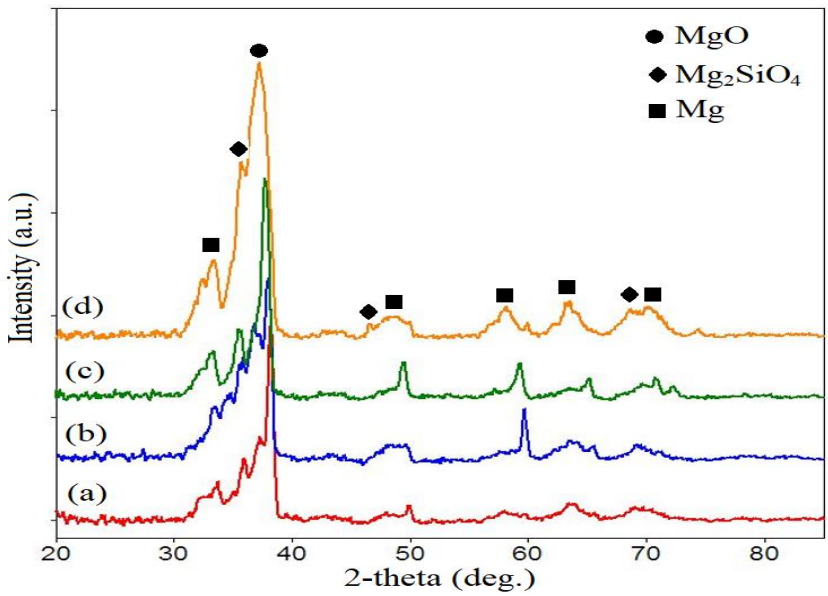

Figure 6.5. XRD analysis of the coatings a) MAO, b) MAO (TiO2), c) MAO (TiN),and d) MAO (TiC).

Figure 6.6 shows the FTIR spectra of the coatings for 6 g/l. The weak band at 3728 cm^{-1} was attributed to the free OH^- stretch vibration of water molecules absorbed on the metallic substrate [78]. The band around 1539 cm^{-1} could be assigned to the formation of Mg_2SiO_4 [79]. The presence of band at 552 cm^{-1} was attributed to the formation of Mg-O [80]. The adsorption peak at 930 cm^{-1} can be assigned to the Si-OH group [81]. The high peak intensities in the MAO (TiC) proves that the coating thickness is the highest among the other coatings.

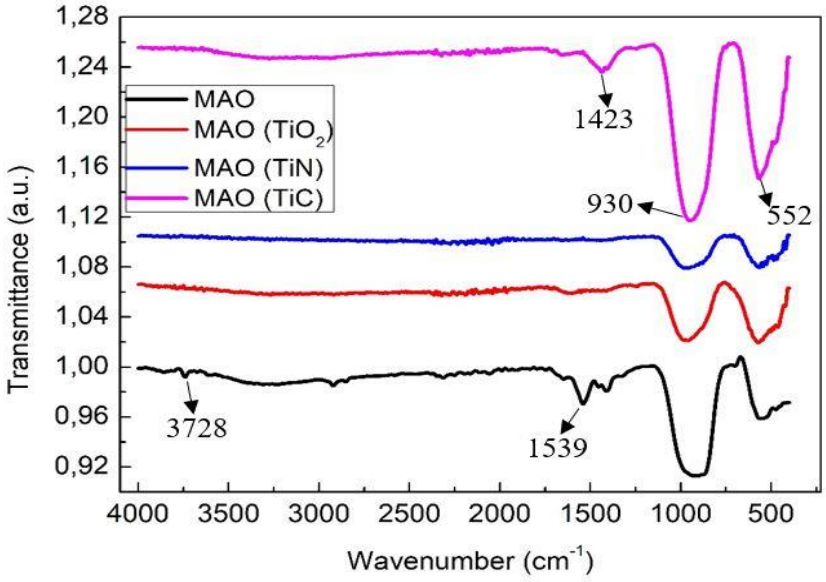

Figure 6.6. FTIR spectra of the coatings.

Figure 6.7 shows the Raman spectra of the coatings. The bands at 227 cm^{-1} and 1439 cm^{-1} are assigned to the presence of MgO for the coatings [82]. The bands appearing at 588 cm^{-1}, 864 cm^{-1}, and 1087 cm^{-1} correspond to stretching vibrations of Si-O. This verifies the presence of Mg_2SiO_4 on the coating structures [83]. For MAO (TiC) coating, the peak intensity increases, and new peaks emerge (1087 cm^{-1}). This proves that MAO (TiC) coating is denser and thicker. From the Raman measurements, no peaks belonging to TiC, TiN and TiO_2 were detected in the structure.

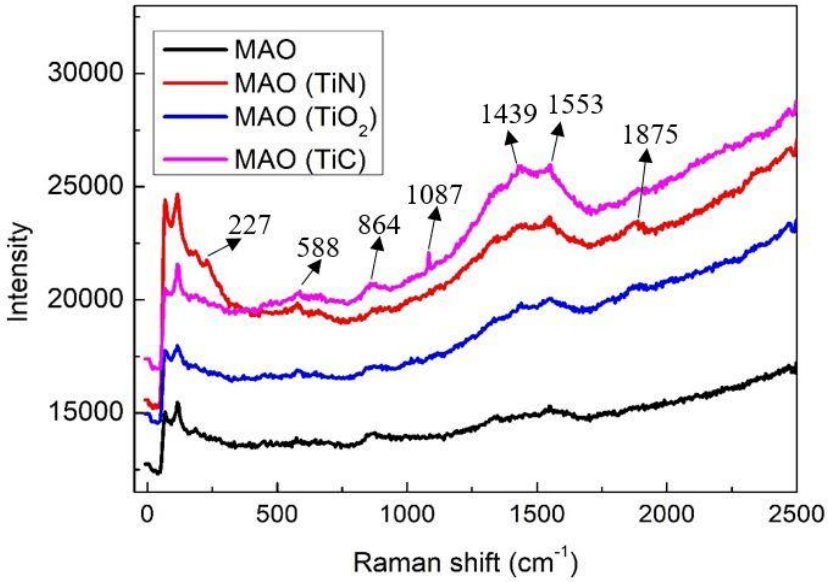

Figure 6.7. Raman spectra of the coatings (6g/l).

Figure 6.8 shows the XPS spectra of the coatings (6 g/l). The survey spectrum of the coatings demonstrated the major peaks assigned to O 1s and Mg 1s. The minor peak of Si 2_S can also be seen for all coatings. This shows that the coatings were primarily composed of Mg, O and Si. The presence of high-intensity C 1s peaks in all coatings is remarkable. This is common for XPS measurements and attributed to the presence of hydrocarbons originated from the environment [84]. For the analysis of the MAO (TiN), the presence of Ti 2p and N 1s is present. This proves the presence of TiN particles on the coating surface. However, there are no Ti 2p peaks for MAO (TiC) and MAO (TiO_2) coatings.

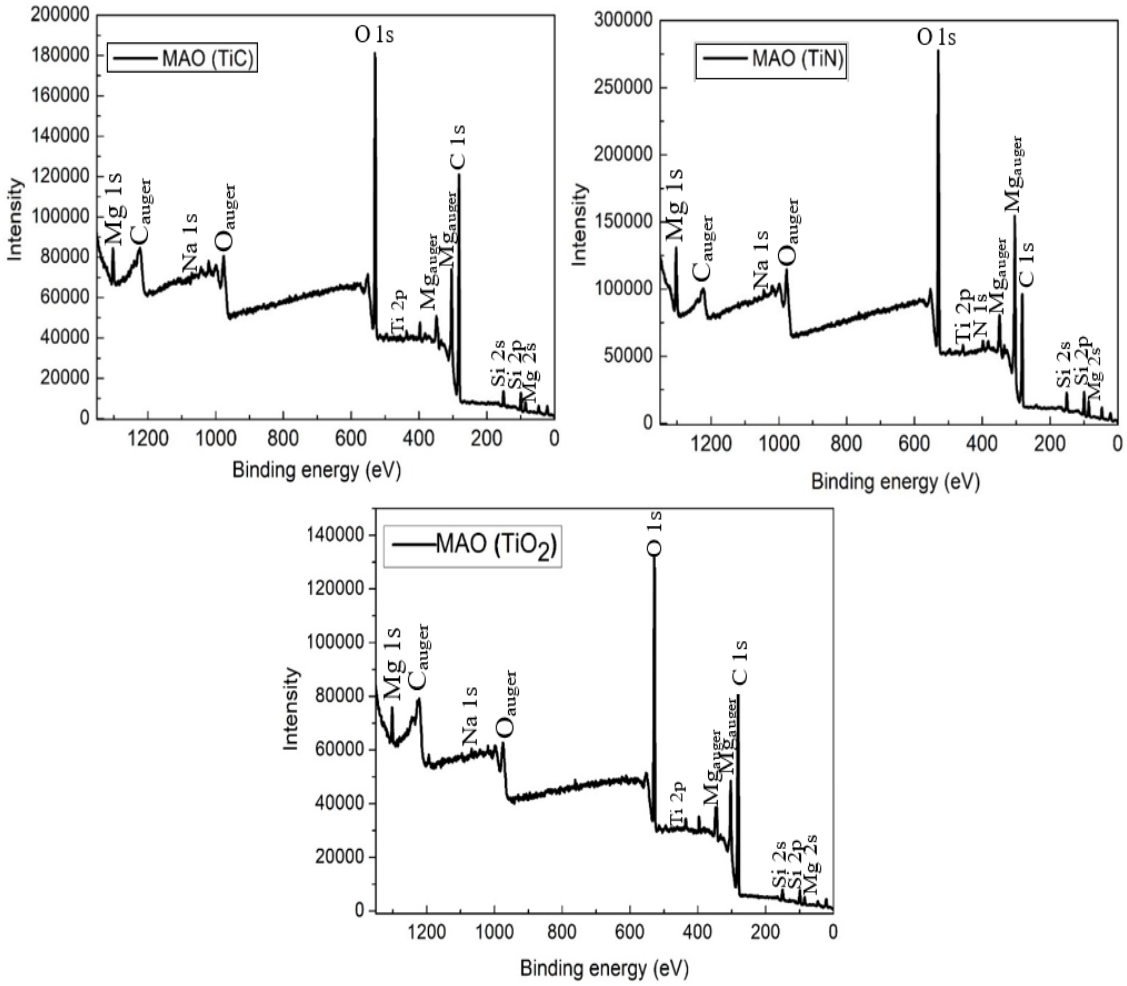

Figure 6.8. XPS spectra of the coatings (6g/l).

6.2. WEAR RESULTS

Figure 6.9 shows the wear rate graphs of all samples under loads of 2, 4 and 6 N for 3 g/l and 6 g/l. It can be seen that the un-coated samples have the highest wear rate for all conditions. The wear rate of the samples decreases in the following order: uncoated sample > MAO > MAO (TiN) > MAO (TiO_2) > MAO (TiC). It is concluded that the maximum wear resistance was obtained for the MAO (TiC) coating. It can also be seen that the coatings for the 6 g/l have higher tribological performance compared to coatings for 3 g/l. Under the load of 6N (for 3g/l), the wear rate of the uncoated sample, MAO, MAO (TiN), MAO (TiO_2), MAO (TiC) was noted to be 0.023, 0.021, 0.020, 0.016 and, 0.015, respectively. Under the load of 6N (for 6g/l), the wear rate of the uncoated sample, MAO, MAO(TiN), MAO(TiO_2), MAO(TiC) was noted to be 0.023, 0.021, 0.019, 0.012, and 0.009, respectively. From the wear results, it is clear that the

incorporation of nanoparticles improved the wear resistance compared to the un-coated sample and coated sample without the particle addition. The increase in wear resistance is attributed to the presence of inertly incorporated particles, leading to high coating hardness and dense layer [85]. It can be said that the higher hardness of the coating surface was obtained due to the high content of particles for 6 g/l. The highest wear resistance of the MAO (TiC) coating can be attributed to the low porosity and roughness [86]. It can be clear that the wear rate of all samples increases with increasing load. Increased load leads to an increase in penetration of the debris of the counterface material. As a result, increased shear loads lead to abrasion and deterioration of wear performance. Several researchers reported that the wear rate increases with increasing applied load for wear studies [87-90].

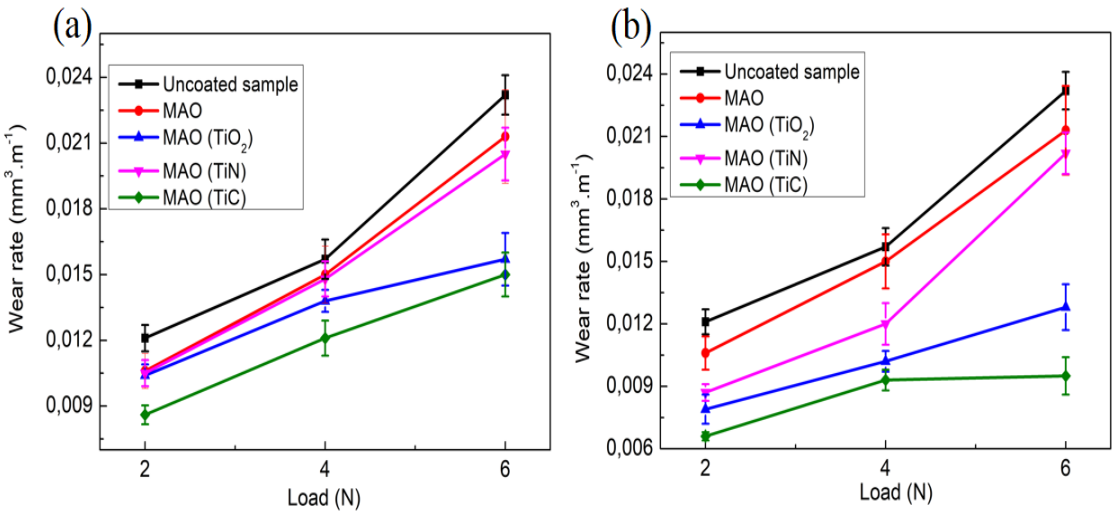

Figure 6.9. Wear rate graphs of the samples: a) 3g/l and b) 6 g/l.

Figure 6.10 shows the worn surface images of the un-coated and coated samples under load of 6N for 6 g/l. It can be seen that the width of wear scar for MAO (TiC) was significantly less than other samples and the width of wear scar for the uncoated sample was the widest. The wear surfaces were found to be consistent with the results of the wear plots in Figure 6.9. Worn surface images were taken at higher magnifications to understand the wear mechanisms. It was observed that the coating layer was removed in the coated materials. During the wear test, visual inspection showed that the coating layer remained on the surface up to a sliding distance of 15 meters. However, from the worn surface images, the smooth surfaces are present for

the coated samples with particle addition. For the enlarged image of the uncoated sample (Figure 6.10a), the crater and wear debris are present on the worn surface. The presence of craters is the result of delamination [91]. For the enlarged image of MAO sample (Figure 6.10b), the scratches are present in the structure. The presence of scratches parallel to the sliding direction verifies the presence of mild abrasive wear mechanism [92, 93]. The wear surface of MAO(TiO_2) appears to be surrounded by wear debris (Figure 6.10c). For the worn surface of MAO (TiN), the cracks and wear debris can be visible. The presence of cracks can be related to the delamination mechanism. During wear, deformation leads to shear deformation near the matrix and cracks occur [94, 95]. For the MAO(TiC), a smooth surface and some wear debris are present on the worn surface. From the worn surface images, it is concluded that the MAO(TiC) has the least damaged area compared to other samples.

Figure 6.11 shows the EDS analysis of the worn surface of MAO(TiC) under load of 6N. For the analysis of area 1, a significant amount of Mg and O was present. This can be attributed to the fracture and deposition of the MgO layer in the coating during the wear test. For the analysis of area 2, the high content Mg and low content O were detected. The presence of O in the structure is due to the formation of frictional heat during the test and the oxidation of the surface [96].

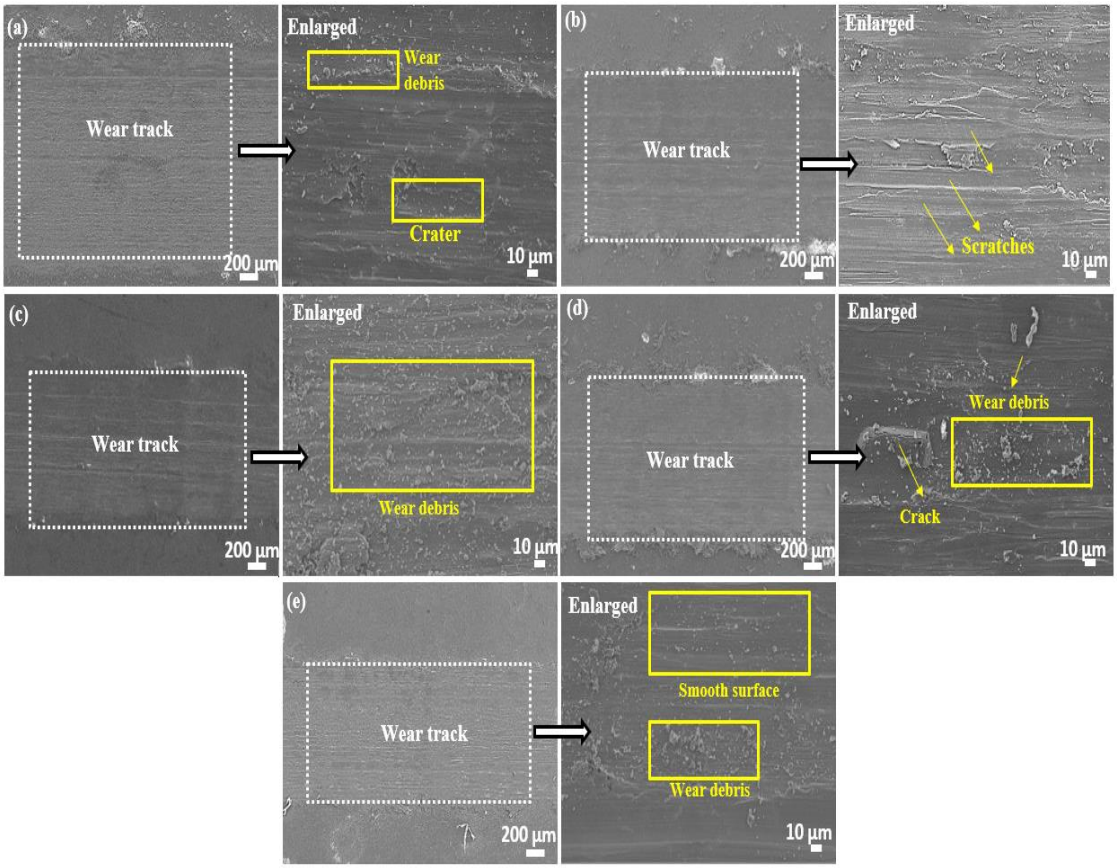

Figure 6.10. Worn surface images of the samples under load of 6 N (6 gr/l): a) un- coated sample, b) MAO, c) MAO(TiO_2), d)MAO(TiN), and e) MAO(TiC).

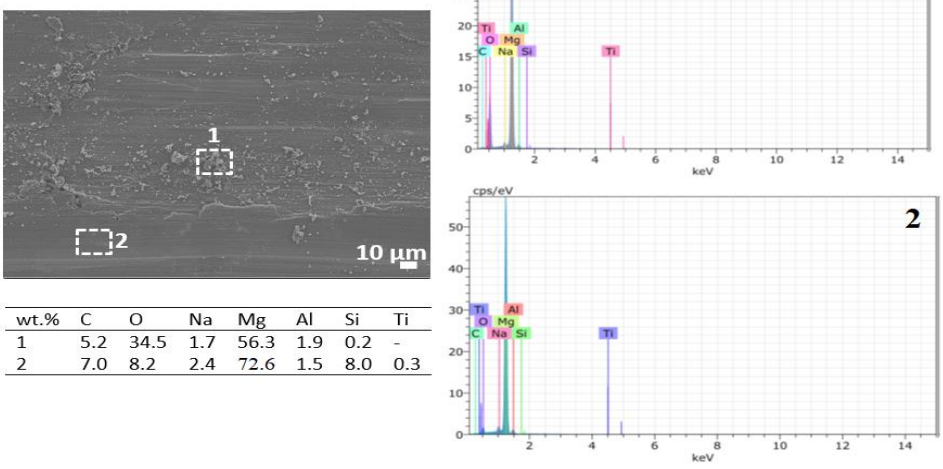

wt.%	C	O	Na	Mg	Al	Si	Ti
1	5.2	34.5	1.7	56.3	1.9	0.2	-
2	7.0	8.2	2.4	72.6	1.5	8.0	0.3

Figure 6.11. EDS analysis of the worn surface of MAO(TiC) under load of 6N.

6.2. CORROSION RESULTS

6.2.1. Potentiodynamic corrosion results

The potentiodynamic test is the most common and basic corrosion test and is used to find the corrosion current and corrosion potential [97, 98]. Figure 6.12 shows the polarization curves of the samples for 3 g/l and 6 g/l. The corrosion potential, corrosion current density, anodic slope and cathodic slope values were obtained from these curves. In addition, the polarization resistance is given according to the Stern-Geary equation [78, 99-101].

$$Rp = \frac{\beta_a \cdot \beta_c}{2.303 \, .i_{corr}(\beta_a + \beta_c)} \tag{6.1}$$

Where β_a is the anodic slope, β_c is the cathodic slope and i_{corr} is the current density.

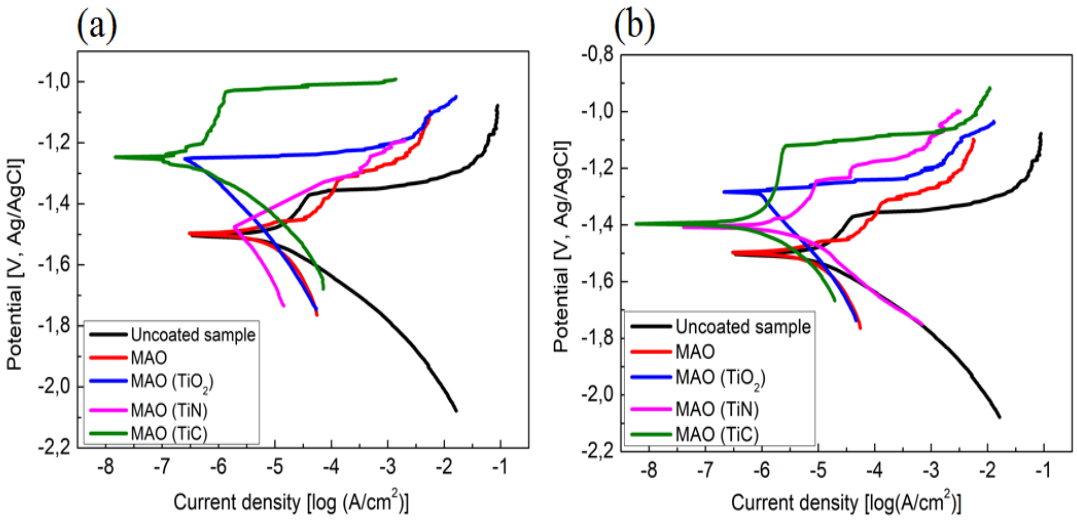

Figure 6.12. Potentiodynamic polarization curves of the samples a) 3g/l and b) 6 g/l.

The electrochemical data obtained from the potentiodynamic corrosion tests are given in Table 6.3 and Table 6.4. From the Tables, it can be seen that the corrosion potential is higher (more noble corrosion potential) for coatings with particle additions compared to the uncoated sample and MAO coating without particle addition. It is well known that the material with higher corrosion potential is less reactive and has the

lowest current density [102-104]. From the tables, it is concluded that the MAO (TiC) has the lowest corrosion current density and the highest polarization resistance. For example, the I_{corr} and Rp of MAO (TiC) was noted to be $27.5x10^{-8}$ (A cm^{-2}) and $105.2x10^{3}$ (Ω cm^{2}) for 3 g/l, respectively. The I_{corr} and Rp of the uncoated sample was noted to be 1.1×10^{-5} and 1.3×10^{3} for 3 g/l, respectively. The highest anti-corrosion property of MAO (TiC) can be attributed to the highest coating thickness of MAO (TiC) compared to other coatings for 6 g/l. Another reason for the high corrosion resistance of MAO (TiC) can be attributed to the fact that the compact coating (with lower porosity) reduces the Mg dissolution (Mg surface activity) during the corrosion test [73]. In addition, it is seen from the tables that the corrosion current densities of the coatings containing 6 g/l are higher and the polarization resistances are lower than the coatings containing 3 g/l. This was attributed to the increased porosity with increasing particle content. The surface became more susceptible to corrosion with increasing porosity, and corrosion accelerates with increasing ion penetration [73, 86].

Table 6.3. Corrosion parameters from the potentiodynamic corrosion tests (3 g/l).

Materials	E_{corr} (V)	β_a (V/dec)	$-\beta_c$ (V/dec)	I_{corr} (A cm^{-2})	Rp (Ω cm^{2})
Uncoated sample	-1.497	0.050	0.153	$1.1x\ 10^{-5}$	1.3×10^{3}
MAO	-1.502	0.135	0.175	$69.2x10^{-7}$	$4.7x10^{3}$
MAO (TiO_2)	-1.252	0.024	0.208	$40.9x10^{-8}$	$22.8\ x10^{3}$
MAO (TiN)	-1.424	0.110	0.290	$22.1x10^{-7}$	$15.6x10^{3}$
MAO (TiC)	-1.249	0.128	0.140	$27.5x10^{-8}$	$105.2x10^{3}$

Table 6.4. Corrosion parameters from the potentiodynamic corrosion tests (6 g/l).

Materials	E_{corr} (V)	β_a (V/dec)	$-\beta_c$ (V/dec)	I_{corr} (A cm^{-2})	Rp (Ω cm^{2})
Uncoated sample	-1.497	0.050	0.153	1.1×10^{-5}	1.3×10^{3}
MAO	-1.502	0.135	0.175	$69.2x10^{-7}$	$4.7x10^{3}$
MAO (TiO_2)	-1.286	0.028	0.228	$9.5x10^{-7}$	$11.3\ x10^{3}$
MAO (TiN)	-1.401	0.093	0.162	$35.4x10^{-7}$	$5.3\ x10^{3}$
MAO (TiC)	-1.396	0.180	0.147	$77.5x10^{-8}$	$45.2\ x10^{3}$

6.2.2. EIS Results

EIS tests were carried out to better understand the corrosion behaviour of the coatings, measure the corrosion resistance numerically and to support the potentiodynamic test results [102]. Figure 6.13 shows the Nyquist plots of the samples for 3 g/l and 6 g/l.

For the uncoated sample, a capacitive loop can be observed. The presence of a capacitive loop is due to the charge transfer process [105]. For the coated samples, similar curves were observed, which shows the presence of a similar corrosion mechanism. However, the corrosion resistance of the coated samples is different from uncoated sample. It is reported that if the capacitive loop is greater, the corrosion resistance is bigger [102]. The MAO (TiC) coating has the biggest capacitive loop compared to other samples, showing excellent corrosion protection. It can be also seen that the radius of the capacitive loop decreases with increasing particle concentration (from 3g/l to 6 g/l). This verifies that the coatings with 6 g/l have lower corrosion protection capacity.

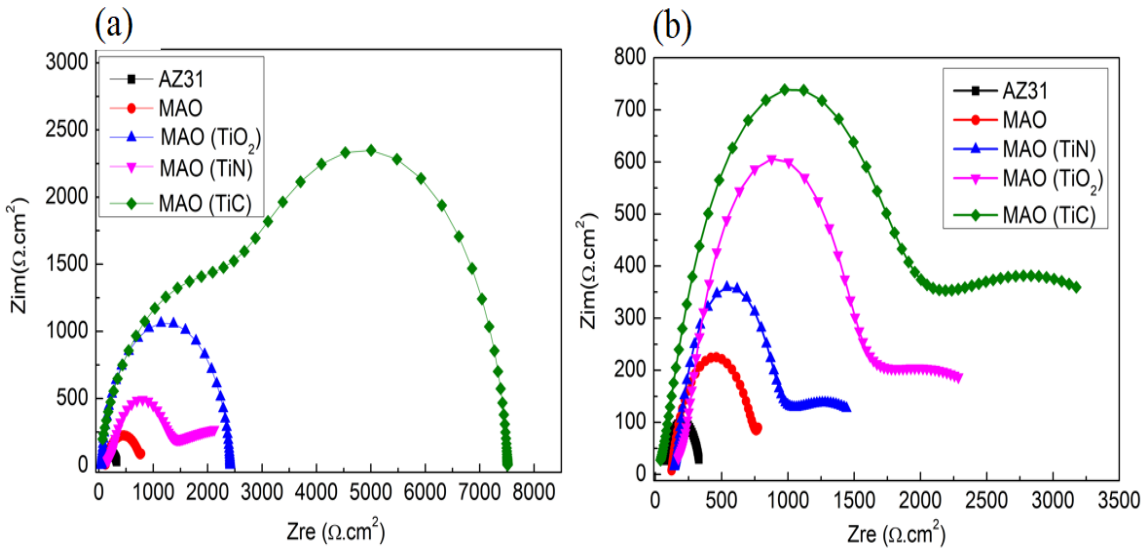

Figure 6.13. Nyquist plots of the samples a) 3g/l and b) 6 g/l

After the EIS tests, the quantitative values are given in Table 6.5 and Table 6.6. In this table, R_s is the resistance of the solution, R_1 and Q_1 are the resistance and capacitance of the porous layer, R_2 and Q_2 are the resistance and capacitance of the dense inner layer, respectively. For all particle additions (3 g/l and 6 g/l), the MAO (TiC) coating has the lowest capacitance and the highest resistance values. This shows that MAO (TiC) has the highest protection capacity. For example, the R_2 values of the MAO (TiC) for 3 g/l and 6 g/l were noted to be 7385 and 2788, respectively. It can be concluded that the coatings with 6 g/l have lower resistance values compared to 3 g/l. This is due to the higher porosity of the coatings containing 6 g/l and the reduced protective effect of the coatings against the Mg substrate NaCl solution [73]. As a

result, the results of the impedance tests were found to be compatible with the potentiodynamic test results.

Table 6.5. EIS fitting results of the samples for 3 g /l.

Materials	R_s ($\Omega.cm^2$)	R_1 ($\Omega.cm^2$)	Q_1 ($\Omega^{-1}.s^n cm^{-2}$)	R_2 ($\Omega.cm^2$)	Q_2 ($\Omega^{-1}.s^n cm^{-2}$)
Uncoated sample	38.1	163	$1.5x10^{-5}$	141	$2.0x10^{-3}$
MAO	119.2	500.3	$5.4x10^{-4}$	651.2	$4.3x10^{-6}$
MAO (TiO_2)	61.9	787.8	$5.8x10^{-7}$	3264	$5.2x10^{-4}$
MAO (TiN)	47.1	1139	$1.2x10^{-6}$	1227	$6.5x10^{-5}$
MAO (TiC)	10.3	3637	$4.5x10^{-8}$	7385	$1.3x10^{-7}$

Table 6.6. EIS fitting results of the samples for 6 g /l.

Materials	R_s ($\Omega.cm^2$)	R_1 ($\Omega.cm^2$)	Q_1 ($\Omega^{-1}.s^n cm^{-2}$)	R_2 ($\Omega.cm^2$)	Q_2 ($\Omega^{-1}.s^n cm^{-2}$)
Uncoated sample	38.1	163	$1.5x10^{-5}$	141	$2.0x10^{-3}$
MAO	119.2	500.3	$5.4x10^{-4}$	651.2	$4.3x10^{-6}$
MAO (TiO_2)	110.1	1002	$5.1x10^{-7}$	1837	$3.5x10^{-4}$
MAO (TiN)	116.5	605.3	$6.7x10^{-7}$	1127	$5.9x10^{-4}$
MAO (TiC)	20.9	1458	$1.0x10^{-6}$	2788	$2.7x10^{-4}$

PART 7
CONCLUSIONS

In this study, the effect of different nanoparticles on the coating morphology, wear, and corrosion of MAO coating of AZ31 alloy was studied. MAO coatings were produced using silicate based electrolyte with the addition of TiC, TiN and TiO_2 particles. The morphology and phase analysis of the coatings were studied using SEM, XRD, FTIR, Raman, XPS. The wear performance of the samples was investigated using reciprocating tests. The corrosion performance was evaluated by potentiodynamic and electrochemical impedance spectroscopy tests. The following results can be drawn:

- The pore size of the coatings decreased with the addition of nanoparticles. The lowest porosity was obtained for 3 g/l in MAO(TiC) coating. However, the surface roughness increased with the addition of nanoparticles.
- The maximum coating thickness was obtained for the MAO(TiC) coating with 6.2 μm.
- XRD, FTIR, RAMAN and XPS analyzes have proven that the coating structures are mostly composed of MgO and Mg_2SiO_4 phases. In addition, SEM and EDS analyzes showed the presence of TiN, TiC and TiO_2 particles in the coating structures.
- From the wear tests, it was determined that the highest wear performance was in the MAO (TiC). In addition, the wear performance of coatings containing 6 g/l was found to be better than coatings containing 3 g/l. The main wear mechanisms were abrasion and delamination. It was observed that the wear surface of the MAO (TiC) is less damaged and smooth.
- According to the potentiodynamic and EIS test results, it was observed that the lowest current density and the highest corrosion resistance were obtained in the MAO (TiC) coating. This proves that coating MAO(TiC) has the highest corrosion protection capacity. In addition, it is concluded that the corrosion

- performance of the coatings decreased when the particle addition increased from 3 g/l to 6 g/l.

REFERENCES

1. Zeng, Z., Nie, J.-F., Xu, S.-W., HJ Davies, C., and Birbilis, N., "Super-formable pure magnesium at room temperature", ***Nature Communications***, 8(1): 1-6 (2017).

2. Zheng, Z., Zhao, M.-C., Tan, L., Zhao, Y.-C., Xie, B., Yin, D., Yang, K., and Atrens, A., "Corrosion behavior of a self-sealing coating containing CeO2 particles on pure Mg produced by micro-arc oxidation", ***Surface and Coatings Technology***, 386125456 (2020).

3. Aydin, F., Sun, Y., Ahlatci, H., and Turen, Y., "Investigation of microstructure, mechanical and wear behaviour of B4C particulate reinforced magnesium matrix composites by powder metallurgy", ***Transactions of the Indian Institute of Metals***, 71(4): 873-882 (2018).

4. Gupta, M., "Magnesium: The Wonder Element for Engineering/Biomedical Applications", ***BoD–Books on Demand***, (2020).

5. King, J., "Magnesium: commodity or exotic?", ***Materials Science and Technology***, 23(1): 1-14 (2007).

6. Aydin, F., Ayday, A., Turan, M. E., and Zengin, H., "Role of graphene additive on wear and electrochemical corrosion behaviour of plasma electrolytic oxidation (PEO) coatings on Mg–MWCNT nanocomposite", ***Surface Engineering***, 36(8): 791-799 (2020).

7. Avedesian, M. M. and Baker, H., "ASM specialty handbook: magnesium and magnesium alloys", ***ASM international***, (1999).

8. Hussein, R. O. and Northwood, D. O., "Production of anti-corrosion coatings on light alloys (Al, Mg, Ti) by plasma-electrolytic oxidation (PEO)", ***Developments in corrosion protection***, 201-239 (2014).

9. Sun, Y., Cevik, E., Turen, Y., Ahlatci, H., Turan, M. E., Aydin, F., and Zengin, H., "Influence of GNPs and B4C reinforcements on mechanical, thermal and wear properties of magnesium matrix composite produced by powder metallurgy", ***Journal of Composite Materials***, 55(26): 3881-3891 (2021).

10. Gupta, M. and Ling, S. N. M., "Magnesium, magnesium alloys, and magnesium composites", ***John Wiley & Sons***, (2011).

11. Mcbride, E. D., "Absorbable metal in bone surgery: a further report on the use of magnesium alloys", ***Journal of the American Medical Association***, 111(27): 2464-2467 (1938).

12. Kulekci, M. K., "Magnesium and its alloys applications in automotive industry", ***The International Journal of Advanced Manufacturing Technology***, 39(9): 851-865 (2008).

13. Staiger, M. P., Pietak, A. M., Huadmai, J., and Dias, G., "Magnesium and its alloys as orthopedic biomaterials: a review", ***Biomaterials***, 27(9): 1728-1734 (2006).

14. Friedrich, H. E. and Mordike, B. L., "Technology of magnesium and magnesium alloys", ***Magnesium Technology: Metallurgy, Design Data, Applications***, 219-430 (2006).

15. Jien-Wei, Y., "Recent progress in high entropy alloys", ***Ann. Chim. Sci. Mat***, 31(6): 633-648 (2006).

16. Ding, Y., Wen, C., Hodgson, P., and Li, Y., "Effects of alloying elements on the corrosion behavior and biocompatibility of biodegradable magnesium alloys: a review", ***Journal of Materials Chemistry B***, 2(14): 1912-1933 (2014).

17. Lyon, P., Wilks, T., and Syed, I., "The influence of alloying elements and heat treatment upon the properties of elektron 21(EV 31 a) alloy", ***Magnesium Technology 2005***, 303-308 (2005).

18. Lu, Y., Zhang, Y., Cong, M., Li, X., Xu, W., and Song, L., "Microstructures, mechanical and corrosion properties of the extruded AZ31-xCaO alloys", ***Materials***, 11(8): 1467 (2018).

19. Calado, L. M., Taryba, M. G., Morozov, Y., Carmezim, M. J., and Montemor, M. F., "Novel smart and self-healing cerium phosphate-based corrosion inhibitor for AZ31 magnesium alloy", ***Corrosion Science***, 170108648 (2020).

20. Wang, P., Gong, Z. Y., Li, H. L., Yang, Q. G., Cao, W. J., Hu, J., Pu, J., Guo, X. Y., and Xiang, D., "Effect of CoSO4 on the characteristics of micro-arc oxidation coatings", ***Surface Engineering***, 36(2): 216-224 (2020).

21. Ghali, E., Dietzel, W., and Kainer, K.-U., "General and localized corrosion of magnesium alloys: a critical review", ***Journal of Materials Engineering and Performance***, 13(1): 7-23 (2004).

22. Hu, R.-G., Zhang, S., Bu, J.-F., Lin, C.-J., and Song, G.-L., "Recent progress in corrosion protection of magnesium alloys by organic coatings", ***Progress in Organic Coatings***, 73(2-3): 129-141 (2012).

23. Ghavidel, N., Allahkaram, S. R., Naderi, R., Barzegar, M., and Bakhshandeh, H., "Corrosion and wear behavior of an electroless Ni-P/nano-SiC coating on AZ31 Mg alloy obtained through environmentally-friendly conversion coating", ***Surface and Coatings Technology***, 382125156 (2020).

24. Sudarshan, T. and Bhaduri, S., "Wear in cylinder liners", ***Wear***, 91(3): 269-279 (1983).

25. Ilanaganar, E. and Anbuselvan, S., "Wear mechanisms of AZ31B magnesium alloy during dry sliding condition", ***Materials Today: Proceedings***, 5(1): 628-635 (2018).

26. Aydin, F. and Sun, Y., "Investigation of wear behaviour and microstructure of hot-pressed TiB2 particulate-reinforced magnesium matrix composites", ***Canadian Metallurgical Quarterly***, 57(4): 455-469 (2018).

27. Gadow, R. and Scherer, D., "Composite coatings with dry lubrication ability on light metal substrates", ***Surface and Coatings Technology***, 151471-477 (2002).

28. Gray, J. and Luan, B., "Protective coatings on magnesium and its alloys—a critical review", ***Journal of Alloys and Compounds***, 336(1-2): 88-113 (2002).

29. Lopes, D. R., Silva, C. L., Soares, R. B., Pereira, P. H. R., Oliveira, A. C., Figueiredo, R. B., Langdon, T. G., and Lins, V. F., "Cytotoxicity and Corrosion Behavior of Magnesium and Magnesium Alloys in Hank's Solution after Processing by High-Pressure Torsion", ***Advanced Engineering Materials***, 21(8): 1900391 (2019).

30. Zheng, T., Hu, Y., Pan, F., Zhang, Y., and Tang, A., "Fabrication of corrosion-resistant superhydrophobic coating on magnesium alloy by one-step electrodeposition method", ***Journal of Magnesium and Alloys***, 7(2): 193-202 (2019).

31. Barajas, J., Joya, J., Durán, K., Hernández-Barrios, C., Coy, A., and Viejo, F., "Relationship between microstructure and formation-biodegradation mechanism of fluoride conversion coatings synthesised on the AZ31 magnesium alloy", ***Surface and Coatings Technology***, 374424-436 (2019).

32. Xiong, P., Yan, J., Wang, P., Jia, Z., Zhou, W., Yuan, W., Li, Y., Liu, Y., Cheng, Y., and Chen, D., "A pH-sensitive self-healing coating for biodegradable magnesium implants", ***Acta Biomaterialia***, 98160-173 (2019).

33. Echeverry-Rendon, M., Duque, V., Quintero, D., Harmsen, M. C., and Echeverria, F., "Novel coatings obtained by plasma electrolytic oxidation to improve the corrosion resistance of magnesium-based biodegradable implants", ***Surface and Coatings Technology***, 35428-37 (2018).

34. Ghasemi, A., Raja, V., Blawert, C., Dietzel, W., and Kainer, K., "The role of anions in the formation and corrosion resistance of the plasma electrolytic oxidation coatings", ***Surface and Coatings Technology***, 204(9-10): 1469-1478 (2010).

35. Srinivasan, P. B., Liang, J., Blawert, C., Störmer, M., and Dietzel, W., "Effect of current density on the microstructure and corrosion behaviour of plasma electrolytic oxidation treated AM50 magnesium alloy", ***Applied Surface Science***, 255(7): 4212-4218 (2009).

36. Song, X., Lu, J., Yin, X., Jiang, J., and Wang, J., "The effect of pulse frequency on the electrochemical properties of micro arc oxidation coatings formed on magnesium alloy", ***Journal of Magnesium and Alloys***, 1(4): 318-322 (2013).

37. Erdil, M. and Aydın, F., "Influence of graphene particles on the wear and corrosion performance of MAO produced AZ31 alloy", ***Fullerenes, Nanotubes and Carbon Nanostructures***, 29(12): 998-1008 (2021).

38. Rakoch, A. and Bardin, I., "Microarc oxidation of light alloys", ***Metallurgist***, 54(5-6): 378 (2010).

39. McNeill, W. and Gruss, L. L., "Anodic film growth by anion deposition in aluminate, tungstate, and phosphate solutions", ***Journal of The Electrochemical Society***, 110(8): 853 (1963).

40. Kaseem, M., Hussain, T., Rehman, Z. U., and Ko, Y. G., "Stabilization of AZ31 Mg alloy in sea water via dual incorporation of MgO and WO3 during micro-arc oxidation", ***Journal of Alloys and Compounds***, 853157036 (2021).

41. Gerasimov, M., Zheltukhin, R., Zhukov, S., Zalavutdinov, R. K., Shcherbakov, A., Epel'Fel'D, A., and Lyudin, V., "The effect of nickel sulfate additives to microarc oxidation electrolytes on the composition and morphology of the surface layer of MAO coatings on VT1-0 titanium And VT5 alloy", ***Protection of Metals and Physical Chemistry of Surfaces***, 51(7): 1170-1175 (2015).

42. Chen, Q., Li, W., Ling, K., and Yang, R., "Effect of Na2WO4 addition on formation mechanism and microstructure of micro-arc oxidation coating on Al-Ti double-layer composite plate", ***Materials & Design***, 190108558 (2020).

43. Hussein, R., Nie, X., and Northwood, D., "Plasma electrolytic oxidation coatings on Mg-alloys for improved wear and corrosion resistance", ***Corrosion: Material Performance and Cathodic Protection***, 99133-134 (2017).

44. Dou, J., Chen, Y., Yu, H., and Chen, C., "Research status of magnesium alloys by micro-arc oxidation: a review", ***Surface Engineering***, 33(10): 731-738 (2017).

45. Darband, G. B., Aliofkhazraei, M., Hamghalam, P., and Valizade, N., "Plasma electrolytic oxidation of magnesium and its alloys: Mechanism, properties and applications", ***Journal of Magnesium and Alloys***, 5(1): 74-132 (2017).

46. Rama Krishna, L. and Sundararajan, G., "Aqueous corrosion behavior of micro arc oxidation (MAO)-coated magnesium alloys: a critical review", ***JOM***, 66(6): 1045-1060 (2014).

47. Farshid, S. and Kharaziha, M., "Micro and nano-enabled approaches to improve the performance of plasma electrolytic oxidation coated magnesium alloys", ***Journal of Magnesium and Alloys***, 9(5): 1487-1504 (2021).

48. Echeverry-Rendon, M., Duque, V., Quintero, D., Robledo, S. M., Harmsen, M. C., and Echeverria, F., "Improved corrosion resistance of commercially pure magnesium after its modification by plasma electrolytic oxidation with organic additives", ***Journal of Biomaterials Applications***, 33(5): 725-740 (2018).

49. Luo, H., Cai, Q., Wei, B., Yu, B., Li, D., He, J., and Liu, Z., "Effect of (NaPO3) 6 concentrations on corrosion resistance of plasma electrolytic oxidation coatings formed on AZ91D magnesium alloy", ***Journal of alloys and compounds***, 464(1-2): 537-543 (2008).

50. Ghasemi, A., Raja, V., Blawert, C., Dietzel, W., and Kainer, K., "Study of the structure and corrosion behavior of PEO coatings on AM50 magnesium alloy by electrochemical impedance spectroscopy", ***Surface and Coatings Technology***, 202(15): 3513-3518 (2008).

51. Barchiche, C.-E., Rocca, E., Juers, C., Hazan, J., and Steinmetz, J., "Corrosion resistance of plasma-anodized AZ91D magnesium alloy by electrochemical methods", ***Electrochimica Acta***, 53(2): 417-425 (2007).

52. Lu, X., Mohedano, M., Blawert, C., Matykina, E., Arrabal, R., Kainer, K. U., and Zheludkevich, M. L., "Plasma electrolytic oxidation coatings with particle additions–A review", ***Surface and Coatings Technology***, 3071165-1182 (2016).

53. Rehman, Z. U. and Choi, D., "Investigation of ZrO2 nanoparticles concentration and processing time effect on the localized PEO coatings formed on AZ91 alloy", ***Journal of Magnesium and Alloys***, 7(4): 555-565 (2019).

54. Lu, X., Blawert, C., Huang, Y., Ovri, H., Zheludkevich, M. L., and Kainer, K. U., "Plasma electrolytic oxidation coatings on Mg alloy with addition of SiO2 particles", ***Electrochimica Acta***, 18720-33 (2016).

55. Wu, D., Liu, X., Lu, K., Zhang, Y., and Wang, H., "Influence of C3H8O3 in the electrolyte on characteristics and corrosion resistance of the microarc oxidation coatings formed on AZ91D magnesium alloy surface", ***Applied Surface Science***, 255(16): 7115-7120 (2009).

56. Wang, S.-y., Si, N.-c., Xia, Y.-p., and Li, L., "Influence of nano-SiC on microstructure and property of MAO coating formed on AZ91D magnesium alloy", ***Transactions of Nonferrous Metals Society of China***, 25(6): 1926-1934 (2015).

57. Zhang, R., Zhang, S., Yang, N., Yao, L., He, F., Zhou, Y., Xu, X., Chang, L., and Bai, S., "Influence of 8-hydroxyquinoline on properties of anodic coatings obtained by micro arc oxidation on AZ91 magnesium alloys", ***Journal of Alloys and Compounds***, 539249-255 (2012).

58. Addepalli, P., Sawangsri, W., and Ghani, S. C., "A qualitative study on cutting tool materials for bone surgeries", ***Materials Today: Proceedings***, 472457-2462 (2021).

59. Wang, H., Zhang, S., Li, Y., and Sun, D., "Bias effect on microstructure and mechanical properties of magnetron sputtered nanocrystalline titanium carbide thin films", ***Thin Solid Films***, 516(16): 5419-5423 (2008).

60. Gupta, P., Fang, F., Rubanov, S., Loho, T., Koo, A., Swift, N., Fiedler, H., Leveneur, J., Murmu, P., and Markwitz, A., "Decorative black coatings on titanium surfaces based on hard bi-layered carbon coatings synthesized by carbon implantation", ***Surface and Coatings Technology***, 358386-393 (2019).

61. Sforza, P. M., "Manned Spacecraft Design Principles", ***Elsevier***, (2015).

62. Zega, B., Kornmann, M., and Amiguet, J., "Hard decorative TiN coatings by ion plating", ***Thin Solid Films***, 45(3): 577-582 (1977).

63. Pierson, H. O., "Handbook of refractory carbides & nitrides: properties, characteristics, processing and applications", ***William Andrew***, (1996).

64. Uddin, G. M., Jawad, M., Ghufran, M., Saleem, M. W., Raza, M. A., Rehman, Z. U., Arafat, S. M., Irfan, M., and Waseem, B., "Experimental investigation of tribo-mechanical and chemical properties of TiN PVD coating on titanium substrate for biomedical implants manufacturing", ***The International Journal of Advanced Manufacturing Technology***, 102(5): 1391-1404 (2019).

65. Tang, S., Gao, S., Hu, S., Wang, J., Zhu, Q., Chen, Y., and Li, X., "Inhibition effect of APCVD titanium nitride coating on coke growth during n-hexane thermal cracking under supercritical conditions", ***Industrial & Engineering Chemistry Research***, 53(13): 5432-5442 (2014).

66. Mashtalyar, D. V., Sinebryukhov, S. L., Imshinetskiy, I. M., Gnedenkov, A. S., Nadaraia, K. V., Ustinov, A. Y., and Gnedenkov, S. V., "Hard wearproof PEO-coatings formed on Mg alloy using TiN nanoparticles", ***Applied Surface Science***, 503144062 (2020).

67. Wold, A., "Photocatalytic properties of titanium dioxide (TiO2)", ***Chemistry of Materials***, 5(3): 280-283 (1993).

68. Association, T. D. M. "*Titanium Dioxide"*, https://tdma.info/what-is-titanium-dioxide/ (2012).

69. Kale, B. M., Wiener, J., Militky, J., Rwawiire, S., Mishra, R., Jacob, K. I., and Wang, Y., "Coating of cellulose-TiO2 nanoparticles on cotton fabric for durable photocatalytic self-cleaning and stiffness", ***Carbohydrate polymers***, 150107-113 (2016).

70. Song, Y., Sun, X., and Liu, Y., "Effect of TiO2 nanoparticles on the microstructure and corrosion behavior of MAO coatings on magnesium alloy", ***Materials and Corrosion***, 63(9): 813-818 (2012).

71. Nasiri Vatan, H. and Adabi, M., "Investigation of tribological behavior of ceramic–graphene composite coating produced by plasma electrolytic

oxidation", ***Transactions of the Indian Institute of Metals***, 71(7): 1643-1652 (2018).

72. Lee, K. M., Lee, B. U., Yoon, S. I., Lee, E. S., Yoo, B., and Shin, D. H., "Evaluation of plasma temperature during plasma oxidation processing of AZ91 Mg alloy through analysis of the melting behavior of incorporated particles", ***Electrochimica Acta***, 676-11 (2012).

73. Daroonparvar, M., Yajid, M. A. M., Yusof, N. M., and Bakhsheshi-Rad, H. R., "Preparation and corrosion resistance of a nanocomposite plasma electrolytic oxidation coating on Mg-1% Ca alloy formed in aluminate electrolyte containing titania nano-additives", ***Journal of Alloys and Compounds***, 688841-857 (2016).

74. Wang, Y., Wang, F., Xu, M., Zhao, B., Guo, L., and Ouyang, J., "Microstructure and corrosion behavior of coated AZ91 alloy by microarc oxidation for biomedical application", ***Applied Surface Science***, 255(22): 9124-9131 (2009).

75. Mohedano, M., Arrabal, R., Mingo, B., Pardo, A., and Matykina, E., "Role of particle type and concentration on characteristics of PEO coatings on AM50 magnesium alloy", ***Surface and Coatings Technology***, 334328-335 (2018).

76. Aydin, F. and Turan, M. E., "The effect of boron nitride on tribological behavior of Mg matrix composite at room and elevated temperatures", ***Journal of Tribology***, 142(1): (2020).

77. Turan, M. E., Sun, Y., Aydın, F., and Akgul, Y., "Influence of multi-wall carbon nanotube content on dry and corrosive wear performances of pure magnesium", ***Journal of Composite Materials***, 52(23): 3127-3135 (2018).

78. Cai, J., Cao, F., Chang, L., Zheng, J., Zhang, J., and Cao, C., "The preparation and corrosion behaviors of MAO coating on AZ91D with rare earth conversion precursor film", ***Applied Surface Science***, 257(8): 3804-3811 (2011).

79. Castellanos, A., Altube, A., Vega, J., García-Lecina, E., Díez, J., and Grande, H., "Effect of different post-treatments on the corrosion resistance and tribological properties of AZ91D magnesium alloy coated PEO", ***Surface and Coatings Technology***, 27899-107 (2015).

80. Pan, Y., He, S., Wang, D., Huang, D., Zheng, T., Wang, S., Dong, P., and Chen, C., "In vitro degradation and electrochemical corrosion evaluations of microarc oxidized pure Mg, Mg–Ca and Mg–Ca–Zn alloys for biomedical applications", ***Materials Science and Engineering: C***, 4785-96 (2015).

81. Zhang, Z.-Q., Zeng, R.-C., Lin, C.-G., Wang, L., Chen, X.-B., and Chen, D.-C., "Corrosion resistance of self-cleaning silane/polypropylene composite coatings on magnesium alloy AZ31", ***Journal of Materials Science & Technology***, 4143-55 (2020).

82. Akram, M. W., Fakhar-e-Alam, M., Atif, M., Butt, A. R., Asghar, A., Jamil, Y., Alimgeer, K., and Wang, Z. M., "In vitro evaluation of the toxic effects of MgO nanostructure in Hela cell line", ***Scientific Reports***, 8(1): 1-11 (2018).

83. Durben, D. J., McMillan, P. F., and Wolf, G. H., "Raman study of the high-pressure behavior of forsterite (Mg2SiO4) crystal and glass", ***American Mineralogist***, 78(11-12): 1143-1148 (1993).

84. Han, B., Yang, Y., Li, J., Deng, H., and Yang, C., "Effects of the graphene additive on the corrosion resistance of the plasma electrolytic oxidation (PEO) coating on the AZ91 magnesium alloy", ***Int. J. Electrochem. Sci***, 139166-9182 (2018).

85. Lu, X., Blawert, C., Kainer, K. U., Zhang, T., Wang, F., and Zheludkevich, M. L., "Influence of particle additions on corrosion and wear resistance of plasma electrolytic oxidation coatings on Mg alloy", ***Surface and Coatings Technology***, 3521-14 (2018).

86. Wang, X., Ju, P., Lu, X., Chen, Y., and Wang, F., "Influence of Cr2O3 particles on corrosion, mechanical and thermal control properties of green PEO coatings on Mg alloy", ***Ceramics International***, 48(3): 3615-3627 (2022).

87. Aydin, F. and Sun, Y., "Microstructure and wear of a sintered composite with a magnesium alloy AZ91 matrix reinforced with ZrO2 particles", ***Metal Science and Heat Treatment***, 61(5): 325-329 (2019).

88. Aydın, F., "Investigation of elevated temperature wear behavior of Al 2024-BN composites using statistical techniques", ***Journal of Materials Engineering and Performance***, 30(11): 8560-8578 (2021).

89. Aydin, F., Sun, Y., and Turan, M. E., "Investigation of microstructure, mechanical and wear behaviour of B4C particulate reinforced AZ91 matrix composites by powder metallurgy", ***Indian Journal of Chemical Technology,*** 26: 351-354 (2019).

90. Kara, I. H. and Incesu, A., "Microstructural, Mechanical, and Tribological Properties of Mg-3Al-1Sn-1Nd-Mn Alloy", ***Journal of Materials Engineering and Performance***, 30(3): 1674-1682 (2021).

91. Aydin, F., "The investigation of the effect of particle size on wear performance of AA7075/Al2O3 composites using statistical analysis and different machine learning methods", ***Advanced Powder Technology***, 32(2): 445-463 (2021).

92. Selvam, B., Marimuthu, P., Narayanasamy, R., Anandakrishnan, V., Tun, K., Gupta, M., and Kamaraj, M., "Dry sliding wear behaviour of zinc oxide reinforced magnesium matrix nano-composites", ***Materials & Design***, 58475-481 (2014).

93. Erden, M. A. and Aydın, F., "Wear and mechanical properties of carburized AISI 8620 steel produced by powder metallurgy", ***International Journal of Minerals, Metallurgy and Materials***, 28(3): 430-439 (2021).

94. Jeyasimman, D., Narayanasamy, R., Ponalagusamy, R., Anandakrishnan, V., and Kamaraj, M., "The effects of various reinforcements on dry sliding wear behaviour of AA 6061 nanocomposites", ***Materials & Design***, 64783-793 (2014).

95. Turan, M. E., Aydin, F., Sun, Y., Zengin, H., and Akinay, Y., "Wear resistance and tribological properties of GNPs and MWCNT reinforced AlSi18CuNiMg alloys produced by stir casting", ***Tribology International***, 164107201 (2021).

96. Aydin, F., Sun, Y., and Emre Turan, M., "The effect of TiB2 content on wear and mechanical behavior of AZ91 magnesium matrix composites produced by powder metallurgy", ***Powder Metallurgy and Metal Ceramics***, 57(9): 564-572 (2019).

97. Gu, Y., Bandopadhyay, S., Chen, C.-f., Guo, Y., and Ning, C., "Effect of oxidation time on the corrosion behavior of micro-arc oxidation produced AZ31 magnesium alloys in simulated body fluid", ***Journal of Alloys and Compounds***, 543109-117 (2012).

98. Aydin, F., Sun, Y., and Emre Turan, M., "Influence of TiC content on mechanical, wear and corrosion properties of hot-pressed AZ91/TiC composites", ***Journal of Composite Materials***, 54(2): 141-152 (2020).

99. Bakhsheshi-Rad, H. R., Abdellahi, M., Hamzah, E., Ismail, A. F., and Bahmanpour, M., "Modelling corrosion rate of biodegradable magnesium-based alloys: The case study of Mg-Zn-RE-xCa (x= 0, 0.5, 1.5, 3 and 6 wt%) alloys", ***Journal of Alloys and Compounds***, 687630-642 (2016).

100. García-Galvan, F. R., Fajardo, S., Barranco, V., and Feliu Jr, S., "Experimental apparent stern–geary coefficients for AZ31B Mg alloy in physiological body fluids for accurate corrosion rate determination", ***Metals***, 11(3): 391 (2021).

101. Demirdal, S. and Aydın, F., "The influence of low-cost eggshell on the wear and electrochemical corrosion behaviour of novel pure Mg matrix composites", ***Materials Chemistry and Physics***, 277125520 (2022).

102. Zhuang, J., Guo, Y., Xiang, N., Xiong, Y., Hu, Q., and Song, R., "A study on microstructure and corrosion resistance of ZrO2-containing PEO coatings formed on AZ31 Mg alloy in phosphate-based electrolyte", ***Applied Surface Science***, 3571463-1471 (2015).

103. Turan, M. E. and Aydin, F., "Wear and corrosion properties of low-cost eggshell-reinforced green AZ91 matrix composites", ***Canadian Metallurgical Quarterly***, 61(2): 155-171 (2022).

104. AYDIN, F. and ERDEN, M. A., "The Investigation of Electrochemical Corrosion Behaviour of Fe Matrix Composites at Room and Elevated Temperatures", ***Düzce Üniversitesi Bilim ve Teknoloji Dergisi***, 8(1): 418-427 (2021).

105. Song, G., Atrens, A., St John, D., Wu, X., and Nairn, J., "The anodic dissolution of magnesium in chloride and sulphate solutions", ***Corrosion science***, 39(10-11): 1981-2004 (1997).

RESUME

Abubaker Ibrahim Elsadawi, a Libyan, was born in 1967 in the city of Misurata in the State of Libya. He completed his primary education in the same city, then in 1990 he obtained a Bachelor's degree in Materials and Mineral Sciences from the University of Tripoli, he studied in English, he is married and has seven children and his mother tongue is Arabic. Between 2015 to 2017, he gets diploma from Atilim University Ankara, Turkey, then in October 2020 Started M. Sc at Faculty of Metallurgy and Materials Engineering at Karabuk University.